PHASE PORTRAITS OF LINEAR TYPE CENTERS OF POLYNOMIAL HAMILTONIAN SYSTEMS WITH HAMILTONIAN FUNCTION OF DEGREE 5 OF THE FORM $H = H_1(x) + H_2(y)$

JAUME LLIBRE, Y. PAULINA MARTÍNEZ, AND CLAUDIO VIDAL

ABSTRACT. We study the phase portraits on the Poincaré disc for all the linear type centers of polynomial Hamiltonian systems of degree 5 with Hamiltonian function $H(x,y) = H_1(x) + H_2(y)$, where $H_1(x) = \frac{1}{2}x^2 + \frac{a_3}{3}x^3 + \frac{a_4}{4}x^4 + \frac{a_5}{5}x^5$ and $H_2(y) = \frac{1}{2}y^2 + \frac{b_3}{3}y^3 + \frac{b_4}{4}y^4 + \frac{b_5}{5}y^5$ as function of the six real parameters a_3, a_4, a_5, b_3, b_4 and b_5 with $a_5 b_5 \neq 0$.

1. Introduction and statement of the main result

Consider the polynomial differential systems in $\mathbb{R}^2$ of the form

$$\dot{x} = P(x,y), \quad \dot{y} = Q(x,y), \tag{1}$$

the dot denotes derivative with respect to an independent real variable t, usually called the *time*. We assume that the origin $(0,0)$ is an equilibrium of system (1).

We say that the origin is a *center* if there exists a neighborhood U of the origin such that all the orbits of system (1) in $U \setminus \{(0,0)\}$ are periodic. Poincaré [23] and Dulac [11] began the study of this type of equilibria, in the present days many questions on the centers remain open.

If the origin of system (1) is a center, then after introducing a linear change of variables and a scaling of the time, system (1) can be carried to one of three normal forms:

$$\dot{x} = -y + P_2(x,y), \quad \dot{y} = x + Q_2(x,y),$$

called a *linear type center*,

$$\dot{x} = y + P_2(x,y), \quad \dot{y} = Q_2(x,y),$$

called a *nilpotent center*,

$$\dot{x} = P_2(x,y), \quad \dot{y} = Q_2(x,y),$$

called a *degenerate center*, where $P_2(x,y)$ and $Q_2(x,y)$ are polynomials without constant and linear terms.

In this work we deal with a particular polynomial differential systems in $\mathbb{R}^2$ of the form

$$\dot{x} = -y + \tilde{P}_1(y), \quad \dot{y} = x + \tilde{P}_2(x), \tag{2}$$

where $\tilde{P}_1(y)$ and $\tilde{P}_2(x)$ are polynomials without constant and linear terms.

The classification of centers of quadratic differential systems started with the works of Dulac [11], Kapteyn [15, 16] and Bautin [4], and the characterization of their phase portraits in the Poincaré disc was due to Vulpe [25]. There are many partial results for the centers of polynomial differential systems of degree larger than 2. Malkin [18], and Vulpe and Sibirsky [26] characterized the linear type centers of the polynomial differential systems with linear and homogeneous nonlinearities of degree 3. The centers for

2010 *Mathematics Subject Classification.* Primary 34C07, Secondary 34C08.
Key words and phrases. Separable Hamiltonian systems, linear type centers, phase portraits, quartic vector field.

the polynomial differential systems with a linear type center at the origin plus homogeneous nonlinearities of degree greater than 3 have not been characterized, but there are some partial results for degrees 4 and 5, see for example Chavarriga and Giné [5, 6]. Recently, the linear type centers and the nilpotent centers of polynomial Hamiltonian systems with nonlinearities of degree 3 were classified by Colak et al. in [7, 8, 9, 10].

In this paper we study the phase portraits in the Poincaré disc of the linear type centers of the polynomial Hamiltonian systems (2) of degree 4. More precisely, we analyze the phase portraits in the Poincaré disc of the Hamiltonian systems

$$\dot{x} = -\frac{\partial H_2}{\partial y} = -y\ \hat{p}(y), \quad \dot{y} = \frac{\partial H_1}{\partial x} = x\ \hat{q}(x), \tag{3}$$

$$\begin{aligned} \hat{p}(y) &= 1 + b_3 y + b_4 y^2 + b_5 y^3, \\ \hat{q}(x) &= 1 + a_3 x + a_4 x^2 + a_5 x^3, \end{aligned} \tag{4}$$

where the Hamiltonian function is the polynomial of degree five

$$H(x, y) = H_1(x) + H_2(y), \tag{5}$$

with

$$H_1(x) = \frac{1}{2}x^2 + \frac{a_3}{3}x^3 + \frac{a_4}{4}x^4 + \frac{a_5}{5}x^5, \quad H_2(y) = \frac{1}{2}y^2 + \frac{b_3}{3}y^3 + \frac{b_4}{4}y^4 + \frac{b_5}{5}y^5,$$

satisfying $a_5^2 + b_5^2 \neq 0$. We note that system (3) is invariant under the symmetry $(x, y, t) \to (y, x, -t)$.

It is known that Hamiltonian systems are very useful in mathematical physics, specially in celestial mechanics, control engineering, biology and other fields. We can find examples of separable Hamiltonians as in (5) in classical books, for example [13] and [1], and more recently some specific examples can be found in relativistic potential or fluid kinetics. In fact Hamiltonian systems appear in relativistic mechanic studying constant periodic oscillators [17], in fluid kinetics the authors of [24] analyze a non trivial Hamiltonian system with separable variables, and in [20] is studied a mechanic Hamiltonian with rational potential. An important work is due to Guillamon and Pantazi in [14], where they present an algorithm to study the type of local phase portrait of the equilibrium points of a separable polynomial Hamiltonian and they analyze the phase portraits of some particular examples.

Our main result is the following one.

Theorem 1. *The global phase portrait in the Poincaré disc of a linear type center of a polynomial Hamiltonian system* (3) *of degree* 4 *is topologically equivalent to:*

(a) *One of the Figures 11 whenever the polynomials* $\hat{p}(y)$ *and* $\hat{q}(x)$ *have either one real root and two complex, or one real root with multiplicity three.*
(b) *One of the Figures 17, 16 if* $\hat{p}(y)$ *(respectively* $\hat{q}(x)$*) has one real root with multiplicity three or one real and two complex, and* $\hat{q}(x)$ *(respectively* $\hat{p}(y)$*) has two real roots with one of them of multiplicity two.*
(c) *One of the Figures 22-26 if* $\hat{p}(y)$ *(respectively* $\hat{q}(x)$*) has one real root with multiplicity three or one real and two complex, and* $\hat{q}(x)$ *(respectively* $\hat{p}(y)$*) has three different real roots.*

In the other cases the local phase portrait in the Poincaré disc is topologically equivalent to:

(d) *One of the Figures 29 if the polynomials* $\hat{p}(y)$ *and* $\hat{q}(x)$ *have two different real roots, one with multiplicity two.*
(e) *One of the Figures 30, if* $\hat{p}(y)$ *(respectively* $\hat{q}(x)$*) has two different real roots one with multiplicity two, and* $\hat{q}(x)$ *(respectively* $\hat{p}(y)$*) has three different real roots.*
(f) *One of the Figures 31 if the polynomials* $\hat{p}(y)$ *and* $\hat{q}(x)$ *have three different real roots.*

This theorem is proved in sections 5, 6, 7, 8, 9 and 10. It is verified that in cases 4, 5 and 6 there exist 9, 12 and 16 finite equilibria, respectively, which can be centers, saddles, cusps or the union of two hyperbolic sectors.

We remark that under the assumptions of statements (a), (b) and (c) we provide the global phase portraits in the Poincaré disc of the Hamiltonian systems (3), but that under the assumptions of statements (d), (e) and (f) we only provide the local phase portraits in the Poincaré disc of the finite and infinite equilibria. This is due to the fact that there are many possible connections between the separatrices of the equilibria and their characterization leads to analyze at least 7! possibilities in each case, which becomes unworkable in this paper.

The main idea of the proof consists in obtaining the description of the local phase portraits of the finite equilibria, in agreement with [14] the phase portrait of the finite equilibria can be saddles, centers, cusps or the union of two hyperbolic sectors. For the infinite equilibria we found that there only exist two nodes on the Poincaré disc with opposite stability. We also characterize the separatrices of the equilibria and analyze the possible connections between them. As a complement we use the energy level to complete the global phase portrait. Finally using symmetry and the Markus-Neumman-Peixoto result (see details in [19]-[21]-[22]), we are able to classify for the Hamiltonian systems (3) all the global phase portraits unless topological equivalence for the statements (a), (b), and (c) in Theorem 1.

In the following three sections we present general results that will be useful in the proof of the statements of Theorem 1. In section 2 there is a characterization of the polynomials $\hat{p}(y)$ and $\hat{q}(x)$ according with their roots. In section 3 we analyze the local phase portraits of all the possible finite equilibria in relation to their eigenvalues and linear matrix. Finally, in section 4 we characterize the infinite equilibria and their stability.

2. Characterization of the roots of the polynomials $\hat{p}(y)$ and $\hat{q}(x)$

In order to prove our main result Theorem 1 we are going to characterize the type and multiplicity of the roots of the polynomials $\hat{p}(y)$ and $\hat{q}(x)$ (note that any root of these polynomials can be zero) defined in (4) as functions of the parameters a_j and b_j with $j = 3, 4, 5$. This characterization will allow to classify the equilibrium points in the finite region.

First we will analyze the polynomial $\hat{p}(y)$ defined in the first equation of (4). Since it is a cubic polynomial we must have: one simple real root and two complex roots, one simple real root and one real root with multiplicity two (namely double root), one root with multiplicity three (we will call it triple real root), or three simple real roots.

In each case it holds that

I. **One simple real root and two complex:** Assuming that $\hat{p}(y)$ has the form $\hat{p}_1(y) = b_5(y - r)(y - (a + ib))(y - (a - ib))$, where r is the real root and $a \pm ib$ are the complex roots, so the parameters of $\hat{p}(y)$ must satisfy

$$b_3 = -\frac{a^2 + b^2 + 2ar}{(a^2 + b^2)r}, \quad b_4 = \frac{2a + r}{(a^2 + b^2)r}, \quad b_5 = -\frac{1}{(a^2 + b^2)r}.$$

II. **One simple real root and one double real root:** Assuming that $\hat{p}(y)$ has the form $\hat{p}_2(y) = b_5(y - r)(y - s)^2$, where r is the simple real root and s is the double real root, so we have

$$b_3 = -\frac{2r + s}{rs}, \quad b_4 = \frac{r + 2s}{rs^2}, \quad b_5 = -\frac{1}{rs^2}.$$

III. **One triple real root:** Assuming that $\hat{p}(y)$ has the form $\hat{p}_3(y) = b_5(y-r)^3$, where r is the triple real root, it is necessary that

$$b_3 = -\frac{3}{r}, \quad b_4 = \frac{3}{r^2}, \quad b_5 = -\frac{1}{r^3}.$$

IV. **Three simple real roots:** Assuming that $\hat{p}(y)$ has the form $\hat{p}_4(y) = b_5(y-r)(y-s)(y-t)$, where $r, s,\ t$ are the real roots, so we must satisfy

$$b_3 = -\frac{rs+rt+st}{rst}, \quad b_4 = \frac{r+s+t}{rst}, \quad b_5 = -\frac{1}{rst}.$$

Analogously, for the polynomial $\hat{q}(x) = (1 + a_3x + a_4x^2 + a_5x^3)$ we have four possibilities for the types of roots. More precisely, we get that if

i) **The roots are ρ and $\alpha \pm \beta i$**, then

$$a_3 = -\frac{\alpha^2+\beta^2+2\alpha\rho}{(\alpha^2+\beta^2)\rho}, \quad a_4 = \frac{2\alpha+\rho}{(\alpha^2+\beta^2)\rho}, \quad a_5 = -\frac{1}{(\alpha^2+\beta^2)\rho}.$$

ii) **The real roots are ρ and σ as double root**, then

$$a_3 = -\frac{2\rho+\sigma}{\rho\sigma},\ a_4 = \frac{\rho+2\sigma}{\rho\sigma^2},\ a_5 = -\frac{1}{\rho\sigma^2},$$

iii) **The triple real root is ρ**, then

$$a_3 = -\frac{3}{\rho},\ a_4 = \frac{3}{\rho^2},\ a_5 = -\frac{1}{\rho^3}.$$

iv) **The real roots are ρ, σ and τ**, then

$$a_3 = -\frac{\rho\sigma+\rho\tau+\sigma\tau}{\rho\sigma\tau}, \quad a_4 = \frac{\rho+\sigma+\tau}{\rho\sigma\tau}, \quad a_5 = -\frac{1}{\rho\sigma\tau}.$$

Using the previous notations for the polynomials $\hat{p}(y)$ and $\hat{q}(x)$, we observe that there are 16 different vector fields associated to (3) according the number of combinations of the possible roots of the polynomials $\hat{p}(y)$ and $\hat{q}(x)$. For future notation, these combinations will be denoted by: I-i, I-ii, I-iii, I-iv, II-i, II-ii, II-iii, II-iv, III-i, III-ii, III-iii, III-iv, IV-i, IV-ii, IV-iii, IV-iv.

Using the above notations the Hamiltonian system (3) can be written as

$$\dot{x} = \frac{1}{\alpha_1\alpha_2\alpha_3}y(y-\alpha_1)(y-\alpha_2)(y-\alpha_3), \quad \dot{y} = \frac{-1}{\beta_1\beta_2\beta_3}x(x-\beta_1)(x-\beta_2)(x-\beta_3), \tag{6}$$

where $\alpha_1, \alpha_2, \alpha_3, \beta_1, \beta_2$ and β_3 are the roots of $\hat{p}(y)$ and $\hat{q}(x)$ which can be real or complex.

Remark 2. *Interchanging the role of x by y in the previous system* (6) *and taking into account the nature of the roots, we can reduce the study of the global phase portraits of the* 16 *systems to study only* 10 *systems. More precisely, the* 10 *cases that we need to analyze in order to describe all possible global phase portraits of the systems* (3) *are: I-i, I-ii, I-iii, I-iv, II-ii, II-iii, II-iv, III-iii, III-iv, IV-iv.*

In this work we are able to do a complete study of the global phase portraits for the following 7 cases: I-i, I-ii, I-iii, I-iv, II-iii, III-iii, III-iv. Furthermore, for the 10 cases we can give a complete study of the local phase portrait for any of the equilibrium points in the finite region as in the infinite one. We do not study the global phase portraits of the cases II-ii, II-iv and IV-iv due to the fact that they exhibit many possible connections of the separatrices between the finite equilibria.

3. Characterization of the finite equilibria

We remake that the origin of system (3) always is a linear type center. So in this section we shall study the local phase portrait of all finite equilibria different from the origin.

Let q be an equilibrium point of systems (3). We say that this equilibrium is *elementary* if some of their two associated eigenvalues λ_1 and λ_2 of the linear part of the vector field is not zero.

The local phase portrait of a finite elementary equilibrium q for a Hamiltonian system is well known, q is a saddle if $\lambda_1\lambda_2 \neq 0$ (which actually only can be $\lambda_1\lambda_2 < 0$), and a center if $\mathrm{Re}\lambda_1 = \mathrm{Re}\lambda_2 = 0$ (for details see [3]). In a Hamiltonian systems in the plane the finite equilibria cannot have elliptic and parabolic sectors, because this type of systems preserves the area. For the vector field (2) we define energy levels as the curves on which its Hamiltonian (5) is constant.

The equilibrium point q is called *nilpotent* if both eigenvalues are zero but the linear part at this point is not the zero matrix. The local phase portrait of a nilpotent equilibrium point can be studied using Theorem 3.5 of [12]. If the equilibrium q of the Hamiltonian system (3) is nilpotent and finite, then it only can be a saddle, a cusp, or a center.

At last, q is called *degenerate or linearly zero* if the Jacobian matrix at the equilibrium point q is identically zero. To study the local phase portraits of a degenerate equilibrium point we use special changes of variables called blow-ups, see for more details Chapter 3 of [12] or [2].

Initially we note that the point $(\tilde{x}, \tilde{y})$ is a finite equilibrium point of system (3) if and only if $H_1'(\tilde{x}) = 0$ and $H_2'(\tilde{y}) = 0$, the linear matrix associated to this equilibrium point is

$$A = \begin{pmatrix} 0 & -H_2''(\tilde{y}) \\ H_1''(\tilde{x}) & 0 \end{pmatrix}.$$

Thus the eigenvalues associated to the equilibrium point $(\tilde{x}, \tilde{y})$ are of the form $\lambda = \pm\sqrt{-H_1''(\tilde{x}) \cdot H_2''(\tilde{y})}$, and we have the following result.

Lemma 3. *A finite equilibria of the system* (3) *is a linear type center if and only if* $H_1''(\tilde{x}) \cdot H_2''(\tilde{y}) > 0$, *is a hyperbolic saddle if and only if* $H_1''(\tilde{x}) \cdot H_2''(\tilde{y}) < 0$, *is a nilpotent equilibrium point if and only if* $H_1''(\tilde{x}) \cdot H_2''(\tilde{y}) = 0$ *and* $H_1''(\tilde{x})^2 + H_2''(\tilde{y})^2 > 0$, *and it is degenerate if and only if* $H_1''(\tilde{x}) = 0$ *and* $H_2''(\tilde{y}) = 0$.

Our next objective is to give the characterization of the nilpotent and degenerate equilibrium points. In order to do this we will use Theorem 3.5 in [12] and the blow-up technique. Since the equilibrium points are the roots of the polynomials $H_1'(x)$ and $H_2'(y)$, it follows that the existence of a nilpotent equilibrium point is equivalent to have that the root $\tilde{x}$ of H_1' is simple and that the root $\tilde{y}$ of H_2' is double or triple, or the root $\tilde{x}$ of H_1' is double or triple and the root $\tilde{y}$ of H_2' is simple. While the equilibrium point $(\tilde{x}, \tilde{y})$ is degenerate, if and only if, the root $\tilde{x}$ of H_1' is double or triple and the root $\tilde{y}$ of H_2' is also double or triple, so in this last case we could have four possibilities or four possible combinations. Let

$$f_1(x) = \frac{\tilde{x}H_1'(x)}{x(x-\tilde{x})}, \quad f_2(y) = \frac{\tilde{y}H_2'(x)}{y(y-\tilde{y})},$$

be auxiliary functions which are well defined at the point $(\tilde{x}, \tilde{y})$ if $\tilde{x}$ is a real root of $\hat{q}(x)$ and $\hat{y}$ is a real root of $\tilde{y}$. Using the previous remarks and notation of system (6) we have the following result.

Lemma 4. *Let* $(\tilde{x}, \tilde{y})$ *be a nilpotent equilibrium point of system* (3), *then its local phase portrait is as follows:*

(1) *If one of the roots* $\tilde{x}$ *or* $\tilde{y}$ *is a double root and the other is simple of* $H_1'(x)$ *and* $H_2'(y)$ *then* $(\tilde{x}, \tilde{y})$ *it is a cusp.*

(2) *If the root $\tilde{x}$ (respectively $\tilde{y}$) is triple and $\tilde{y}$ (respectively $\tilde{x}$) is simple of $H_1'(x)$ and $H_2'(y)$ then $(\tilde{x},\tilde{y})$ it is a saddle if $f_1(\tilde{x})>0$ (respectively $f_2(\tilde{y})>0$), and it is a center if $f_1(\tilde{x})<0$ (respectively $f_2(\tilde{y})<0$).*

Proof. First we are going to study the nilpotent equilibria $(\tilde{x},\tilde{y})$ when $\tilde{x}$ is a simple root of $H_1'(x)$ and $\tilde{y}$ is a double root of $H_2'(y)$ (the analysis in the case where $\tilde{x}$ is a double root of $H_1'(x)$ and $\tilde{y}$ is a simple root of $H_2'(y)$ is similar). Since we can write system (3) in the form (6), we have that $\alpha_1=\alpha_2=\tilde{y}$ and $\beta_1=\tilde{x}$, then we translate this equilibrium to the origin through the change of variables $(x,y)\to(x+\tilde{x},y+\tilde{y})$ and system (6) becomes

$$
\begin{aligned}
x' &= \left(\frac{1}{\alpha_3}-\frac{1}{\tilde{y}}\right)y^2+\left(\frac{2}{\tilde{y}\alpha_3}-\frac{1}{\tilde{y}^2}\right)y^3+\frac{1}{\tilde{y}^2\alpha_3}y^4,\\
y' &= \left(-\frac{\tilde{x}^2}{\beta_2\beta_3}+\frac{\tilde{x}}{\beta_3}+\frac{\tilde{x}}{\beta_3}-1\right)x+\left(-\frac{3\tilde{x}}{\beta_2\beta_3}-\frac{1}{\tilde{x}}+\frac{2}{\beta_2}+\frac{2}{\beta_3}\right)x^2+\\
&\quad \frac{(-3\tilde{x}+\beta_2+\beta_3)}{\tilde{x}\beta_2\beta_3}x^3-\frac{1}{\tilde{x}\beta_2\beta_3}x^4.
\end{aligned}
\tag{7}
$$

We write the linear part of this system at the origin in its real Jordan normal form, we apply the change of variables $(x,y)=P(u,v)$ with the matrix $P=\begin{pmatrix}0 & \frac{\beta_2\beta_3}{(\beta_2-\tilde{x})(\tilde{x}-\beta_3)}\\ 1 & 0\end{pmatrix}$ and system (7) takes the form

$$
\begin{aligned}
u' &= v+\frac{\beta_2\beta_3(-3\tilde{x}^2+2\tilde{x}(\beta_2+\beta_3)-\beta_2\beta_3)}{\tilde{x}(\tilde{x}-\beta_2)^2(\tilde{x}-\beta_3)^2}v^2-\frac{\beta_2^2\beta_3^2(-3\tilde{x}+\beta_2+\beta_3)}{\tilde{x}(\tilde{x}-\beta_2)^3(\tilde{x}-\beta_3)^3}v^3-\frac{\beta_2^3\beta_3^3}{\tilde{x}(\tilde{x}-\beta_2)^4(\tilde{x}-\beta_3)^4}v^4,\\
v' &= -\frac{(\tilde{y}-\alpha_3)(\tilde{x}-\beta_2)(\tilde{x}-\beta_3)}{\tilde{y}\alpha_3\beta_2\beta_3}u^2+\frac{(2\tilde{y}-\alpha_3)(\beta_2-\tilde{x})(\tilde{x}-\beta_3)}{\tilde{y}^2\alpha_3\beta_2\beta_3}u^3+\frac{(\beta_2-\tilde{x})(\tilde{x}-\beta_3)}{\tilde{y}^2\alpha_3\beta_2\beta_3}u^4.
\end{aligned}
$$

Using the notation and the results of Theorem 3.5 in [12], we have $F(x)=-\frac{(\tilde{y}-\alpha_3)(\tilde{x}-\beta_2)(\tilde{x}-\beta_3)}{\tilde{y}\alpha_3\beta_2\beta_3}u^2+O(u^3)$ and $G(x)\equiv 0$, consequently $m=2$ (even) and the equilibrium is a cusp.

To prove of the statement (b) of the lemma we suppose that $\tilde{x}$ is a triple root of $H_1'(x)$ and $\tilde{y}$ is a simple root of $H_2'(y)$ (the analysis of the other case is similar). Translating the equilibrium $(\tilde{x},\tilde{y})$ of system (6) to the origin we get the system

$$
\begin{aligned}
x' &= \frac{\alpha_2\alpha_3+\tilde{y}^2-\alpha_2\tilde{y}-\alpha_3\tilde{y}}{\alpha_2\alpha_3}y+\frac{-2(\alpha_2+\alpha_3)+3\tilde{y}^2+\alpha_2\alpha_3}{\alpha_2\alpha_3\tilde{y}}y^2+\frac{-\alpha_2-\alpha_3+3\tilde{y}}{\alpha_2\alpha_3\tilde{y}}y^3+\frac{1}{\alpha_2\alpha_3\tilde{y}}y^4,\\
y' &= -\frac{1}{\tilde{x}^2}x^3-\frac{1}{\tilde{x}^3}x^4.
\end{aligned}
\tag{8}
$$

Again we write system (8) such that the linear part at the origin be in their real Jordan normal form, this is achieved applying the change of variables $(x,y)=P(u,v)$ with $P=\begin{pmatrix}1 & 0\\ 0 & \frac{\alpha_2\alpha_3}{(\tilde{y}-\alpha_2)(\tilde{y}-\alpha_3)}\end{pmatrix}$, so system (8) assumes the form

$$
\begin{aligned}
u' &= v+\frac{\alpha_2\alpha_3\left(\alpha_2\alpha_3+3(\tilde{y})^2-2\tilde{y}(\alpha_2+\alpha_3)\right)}{\tilde{y}(\tilde{y}-\alpha_2)^2(\tilde{y}-\alpha_3)^2}v^2-\frac{\alpha_2^2\alpha_3^2(\alpha_2+\alpha_3-3\tilde{y})}{\tilde{y}(\tilde{y}-\alpha_2)^3(\tilde{y}-\alpha_3)^3}v^3-\frac{\alpha_2^2\alpha_3^2(\alpha_2+\alpha_3-3\tilde{y})}{\tilde{y}(\tilde{y}-\alpha_2)^3(\tilde{y}-\alpha_3)^3}v^4,\\
v' &= -\frac{(\tilde{y}-\alpha_2)(\tilde{y}-\alpha_3)}{\alpha_2\alpha_3\rho^2}u^3-\frac{(\tilde{y}-\alpha_2)(-\alpha_3)}{\alpha_2\alpha_3\tilde{x}^3}u^4.
\end{aligned}
$$

Again using the notation and the results of Theorem 3.5 in [12] we have that $F(x)=\frac{(\tilde{y}-\alpha_2)(\tilde{y}-\alpha_3)}{\alpha_2\alpha_3\rho^2}u^3+O(u^4)$ and $G(x)\equiv 0$, thus $m=3$ (odd) and $a_3=\frac{(-\tilde{y}+\alpha_2)(\tilde{y}-\alpha_3)}{\alpha_2\alpha_3\tilde{x}^2}$. Therefore if $a_3>0$ the equilibrium $(\tilde{x},\tilde{y})$ is a saddle and if $a_3<0$ the equilibria is a center. In case that the triple root is $\tilde{y}$ of $H_2'(y)$ the

coefficient a_3 takes the form $\frac{(\beta_2-\tilde{x})(-\beta_3+\tilde{x})}{\tilde{y}^2\beta_2\beta_3}$ and the conclusion is the same. This completes the proof of the lemma.

□

Lemma 5. *Let $(\tilde{x},\tilde{y})$ be a degenerate equilibrium point of system (3), then its local phase portrait is as follows:*

1. *If $\tilde{x}$ and $\tilde{y}$ are double roots of $H_1'(x)$ and $H_2'(y)$, then $(\tilde{x},\tilde{y})$ is the union of two hyperbolic sectors (see Figure 2).*
2. *If $\tilde{x}$ and $\tilde{y}$ are triple roots of $H_1'(x)$ and $H_2'(y)$, then it is a center.*
3. *If one of roots $\tilde{x}$ or $\tilde{y}$ is double and the other is triple of $H_1'(x)$ and $H_2'(y)$, then it is a cusp.*

Proof. An equilibrium $(\tilde{x},\tilde{y})$ is degenerate if $\tilde{x}$ and $\tilde{y}$ are double or triple roots of $H_1'(x)$ and $H_2'(y)$. To prove statement (a) we consider that $\tilde{x}$ and $\tilde{y}$ are double roots of $H_1'(x)$ and $H_2'(y)$. So the associated system (3), after translating the degenerate equilibrium to the origin, takes the form

$$x' = \frac{(\tilde{y}+y)(\tilde{y}-\alpha_3+y)y^2)}{\tilde{y}^2\alpha_3}, \quad y' = -\frac{(\tilde{x}+x)(\tilde{x}-\beta_3+x)x^2)}{\tilde{x}^2\beta_3}. \tag{9}$$

Next we apply the directional blow-up $(x,y)\mapsto(x,w)$ with $y = w\,x$, and after eliminating the common factor x we arrive to the system

$$\begin{aligned} x' &= \frac{w^2x(\tilde{y}+wx)(\tilde{y}+wx-\alpha_3)}{\tilde{y}^2\alpha_3}, \\ w' &= -\frac{w^3(\tilde{y}+wx)(\tilde{y}+wx-\alpha_3)}{\tilde{y}^2\alpha_3} - \frac{(\tilde{x}+x)(\tilde{x}+x-\beta_3)}{\tilde{x}^2\beta_3}. \end{aligned} \tag{10}$$

System (10) has one equilibrium with $x=0$ and $\tilde{w} = -\frac{(\tilde{y}\alpha_3(\beta_3-\tilde{x})^{1/3}}{(\beta_3\tilde{x}(\alpha_3-\tilde{x}))^{1/3}}$, with eigenvalues $\lambda_1 = 3\kappa$, $\lambda_2 = -\kappa$ where $\kappa = \frac{-\beta_3(\beta_3-\tilde{x})^2\tilde{x}(\tilde{y}-\alpha_3)^{1/3}}{\tilde{x}\beta_3(\tilde{y}\alpha_3)^{1/3}} \neq 0$, so it is a saddle. In Figure 1 we can see the phase portrait of the origin of system (10) according to the signs of $\tilde{w}$ and κ. We can obtain the local phase portrait at the origin of system (9) going back through the blow-up and considering the vector field over the y-axis given by $x'|_{x=0} = \frac{(\tilde{y}+y)(\tilde{y}-\alpha_3+y)y^2)}{\tilde{y}\alpha_3}$. After reconstructing the local phase portrait of the origin of system (9) we get one shown in Figure 2.

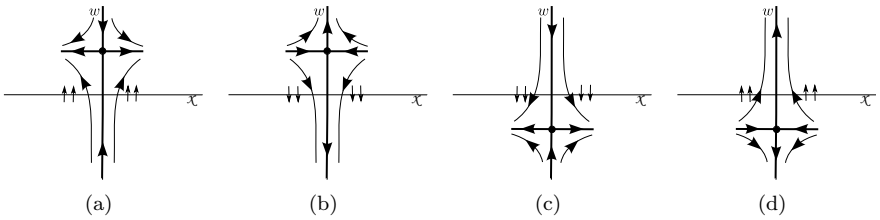

(a) (b) (c) (d)

FIGURE 1. Phase portrait in a neighborhood of the w-axis of system (10). (a) $\tilde{w} > 0$ and $\kappa > 0$. (b) $\tilde{w} > 0$ and $\kappa < 0$. (c) $\tilde{w} < 0$ and $\kappa > 0$. (d) $\tilde{w} < 0$ and $\kappa < 0$.

To prove the second statement of the lemma we have that $\tilde{x}$ and $\tilde{y}$ are triple roots of $H_1'(x)$ and $H_2'(y)$, respectively, the associated system (3), after translating the degenerate equilibrium to the origin is

$$x' = \frac{1}{\tilde{y}^3}(\tilde{y}+y)y^3, \quad y' = \frac{-1}{\tilde{x}^3}(\tilde{x}+x)x^3. \tag{11}$$

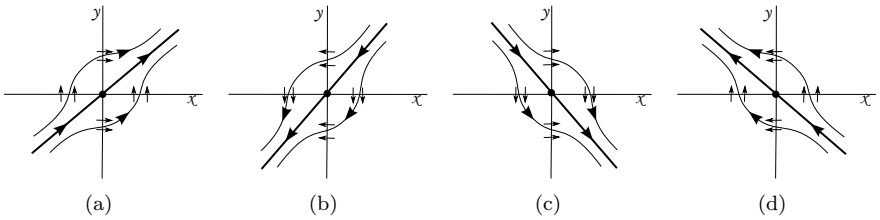

FIGURE 2. Local phase portrait at the origin of system (9). (a) $\tilde{w} > 0$ and $\kappa > 0$. (b) $\tilde{w} > 0$ and $\kappa < 0$. (c) $\tilde{w} < 0$ and $\kappa > 0$. (d) $\tilde{w} < 0$ and $\kappa < 0$.

We apply the directional blow-up $(x, y) \mapsto (x, w)$ with $y = w\,x$, and after eliminating the common factor x^2, we arrive to the system

$$x' = \frac{1}{\tilde{y}^3} x w^3 (\tilde{y} + wx), \quad w' = -\frac{1}{\tilde{x}^2} - \frac{w^4}{\tilde{y}^2} + \left(-\frac{1}{\tilde{x}^3} - \frac{w^5}{\tilde{y}^3} \right) x. \tag{12}$$

System (12) has no real equilibria on $x = 0$, so we analyze the vector field (12) over the axes and we have $x'|_{x=0} = 0$, $x'|_{w=0} = 0$, $w'|_{x=0} = -\frac{1}{\rho^2} - \frac{w^4}{r^2} < 0$ and $w'|_{w=0} = -\frac{x+\tilde{x}}{\tilde{x}^3} < 0$. So the local phase portrait at the origin of system (12) is as in Figure 3 (a). We can reconstruct the local phase portrait at the origin of system (11) going back through the blow-up considering the flow of the vector field over the y-axis $x'|_{x=0} = \frac{(\tilde{y}+y)(\tilde{y}-\alpha_3+y)y^2}{\tilde{y}\alpha_3}$, then the local phase portrait at the origin of system (11) is a center as is shown in Figure 3 (b).

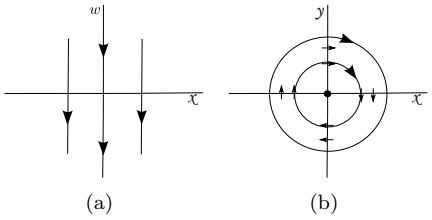

FIGURE 3. Blow-up at the origin of system (11). (a) Local phase portrait at the origin of the system (12). (b) Local phase portrait at the origin of the system (11).

In the last statement of the lemma we have that one root is triple and the other is double. We study first the case when $\tilde{x}$ is a double root of $H_1'(x)$ and $\tilde{y}$ is a triple root of $H_2'(y)$. Thus the associated system after translating the degenerate equilibrium to the origin is

$$x' = \frac{1}{\tilde{y}^2\alpha_3} y^2 (\tilde{y} + y)(\tilde{y} + y - \alpha_3), \quad y' = \frac{-1}{\tilde{x}^3} (\tilde{x} + x) x^3. \tag{13}$$

Here we apply the directional blow-up $(x, y) \mapsto (x, w)$ with $y = w\,x$, and after eliminating the common factor x we arrive to the system

$$\begin{aligned} x' &= \frac{1}{\tilde{y}^2\alpha_3} x w^2 (\tilde{y} + wx)(\tilde{y} + wx - \alpha_3), \\ w' &= \frac{w^3}{\tilde{y}} - \frac{w^3}{\alpha_3} + \left(-\frac{1}{\tilde{x}^2} + \frac{w^4}{\tilde{y}^2} - \frac{2w^4}{\tilde{y}\alpha_3} \right) x - \left(\frac{1}{\tilde{x}^3} + \frac{w^5}{\tilde{y}^2\alpha_3} \right) x^2. \end{aligned} \tag{14}$$

For $x = 0$ the origin is the unique equilibrium of system (14), and this equilibrium is nilpotent. To understand the local phase portrait of $(0,0)$ of system (14) we do the change of variables $(x, w) \mapsto P(u, v)$ with the matrix $P = \begin{pmatrix} 0 & -\rho^2 \\ 1 & 0 \end{pmatrix}$, thus we arrive to the system

$$\begin{aligned} u' &= \frac{u^3}{r} - \frac{u^3}{\alpha_3} + \left(-\frac{\tilde{x}^2 u^4}{\tilde{y}^2} + \frac{2\tilde{x}^2 u^4}{\tilde{y}\alpha_3} + 1 \right) v + \left(-\tilde{x} - \frac{\tilde{x}^4 u^5}{\tilde{y}^2 \alpha_3} \right) v^2, \\ v' &= \frac{1}{\tilde{y}^2 \alpha_3} u^2 v \left(\tilde{x}^2 uv - \tilde{y} \right) \left(-\tilde{y} + \tilde{x}^2 uv + \alpha_3 \right). \end{aligned}$$

Using the notation and the results of Theorem 3.5 in [12] we have $F(x) = \frac{(\tilde{y}-\alpha_3)^2}{\tilde{y}^2\alpha_3^2)} u^5 + O(u^6)$ and $G(x) = \frac{2(\tilde{y}-\alpha_3)}{\tilde{y}\alpha_3} u^2 + O(u^3)$. Thus $n = 2$ (even), $m = 5$ (odd) and $a > 0$, then $(0,0)$ in (14) is a saddle as is shown in Figure 4(a) if $(\alpha_3 - \tilde{y})/(\alpha_3 \tilde{y}) > 0$, or in Figure 5(a) if $(\alpha_3 - \tilde{y})/(\alpha_3 \tilde{y}) < 0$. Going back through the blow-up and considering the flow over the y-axis, we found that the local phase portrait at the origin of system (13) is as shown in Figure 4(b) for $(\alpha_3 - \tilde{y})/(\alpha_3 \tilde{y}) > 0$, or is the one of Figure 5(b) if $(\alpha_3 - \tilde{y})/(\alpha_3 \tilde{y}) < 0$, that is, the equilibrium is a cusp.

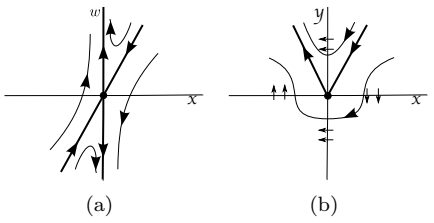

FIGURE 4. Assume $(\alpha_3 - \tilde{y})/(\alpha_3 \tilde{y}) > 0$. (a) Local phase portrait in a neighbourhood at the w-axis of system (14). (b) Local phase portrait at the origin of system (13).

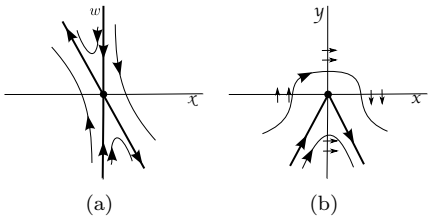

FIGURE 5. Assume $(\alpha_3 - \tilde{y})/(\alpha_3 \tilde{y}) < 0$. (a) Local phase portrait in a neighbourhood at the w-axis of system (14). (b) Local phase portrait at the origin of system (13).

Now assume that $\tilde{x}$ is a triple root of $H_1'(x)$ and $\tilde{y}$ is a double root of $H_2'(y)$, then the Hamiltonian system (6) takes the form

$$x' = \frac{1}{\tilde{y}^3} y(y - \tilde{y}), \quad y' = \frac{-1}{\tilde{x}^2 \beta_3} x(x - \tilde{x})^2 (x - \beta_3). \tag{15}$$

Applying the directional blow-up $(x, y) \mapsto (x, w)$ with $y = w\,x$, and eliminating the common factor x we arrive to the system

$$x' = \frac{w^3 x^2 (\tilde{y} + wx)}{\tilde{y}^3}, \quad w' = -\frac{1}{\beta_3} + \frac{1}{\tilde{x}} + \left(-\frac{w^4}{\tilde{y}^2} + \frac{1}{\tilde{x}^2} - \frac{2}{\beta_3 \tilde{x}^2} \right) x + \left(-\frac{w^5}{\tilde{y}^3} - \frac{1}{\beta_3 \tilde{x}^2} \right) x^2. \tag{16}$$

System (16) does not have equilibria with $x = 0$, so we analyze the behavior of the vector field in a neighborhood of the origin, for this we consider $\tilde{y} > 0$ and $0 < \tilde{x} < \beta_3$ (the other cases, when $y < 0$ or for other order of $\tilde{x}$ and β_3, are similar), here the vector field increases in the w-direction and cut orthogonality the x-axis. Furthermore the w-axis is invariant and the flow of system (16) is as in Figure 6(a). Going back through the blow-up we can obtain the local phase portrait of the origin of system (15) after analyzing the vector field over the axes, that is $x'|_{x=0} = y(y-\tilde{y})/\tilde{y}^3$ and $x'|_{y=0} = 0$, we get $x'|_{x=0} > 0$ if $y > 0$ and $x'|_{x=0} < 0$ if $y < 0$. Thus by the continuity of the flow its local phase portrait close at origin implies that one orbit located in the first quadrant and one orbit located in the fourth quadrant must connect with the equilibrium at the origin, thus the equilibrium is a cusp as it is shown in Figure 6(b).

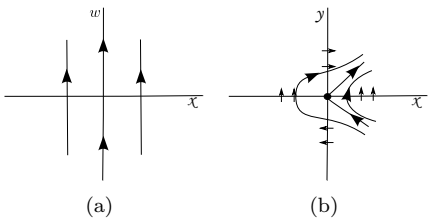

FIGURE 6. Blow-up of the origin of system (15). (a) Local phase portrait at in a neighborhood of the w-axis of system (16). (b) Local phase portrait at the origin of system (15).

We have already proved the third statement of the lemma, so this completes its proof. □

4. Characterization of the infinite equilibria

In order to study the equilibrium points at the infinity we are going to follow the classic technique of the Poincaré compactification (see for details in chapter 5 in [12]) First we write system (3) in the local chart U_1 (where $U_i = \{y \in \mathcal{S}^2 : y_i > 0\}$ is a local chart of the Sphere $\mathcal{S}^2 = \{y = (y_1, y_2, y_3) \in \mathbb{R}^3 : y_1^2 + y_2^2 + y_3^2 = 1)\}$) and we get

$$\begin{aligned} \dot{z}_1 &= a_5 + b_5 z_1^5 + z_2[a_4 + b_4 z_1^4 + z_2(a_3 + b_3 z_1^3 + z_2 + z_1^2 z_2)], \\ \dot{z}_2 &= z_1 z_2[b_5 z_1^3 + b_4 z_1^2 z_2 + b_3 z_1 z_2^2 + z_2^3]. \end{aligned} \tag{17}$$

So at infinity, i.e. at $z_2 = 0$ system (17) has a unique equilibrium point given by $P = (-(a_5/b_5)^{1/5}, 0)$. The eigenvalues of the linear part of system (17) at P are $\lambda_1 = (a_5^4 b_5)^{1/5}$ and $\lambda_2 = 5(a_5^4 b_5)^{1/5}$. Therefore the infinite equilibrium P is a stable node if $b_5 < 0$, or is an unstable node if $b_5 > 0$. As the degree of system (3) is 4 (even), we have that there exists a node in V_1 with the opposite stability of P. On the other hand on the local chart U_2 it is easily verified that the origin is not an equilibrium. This completes the analysis of the equilibria in the infinite region.

5. Proof of Theorem 1 statement (a)

In this section we are going to prove statement (a) of Theorem 1. We consider that the polynomials $\hat{p}(y)$ and $\hat{q}(x)$ have one real root and two complex or one real root with multiplicity three. By Remark 2 it is sufficient to study the cases I-i, I-iii and III-iii. We are going to analyze these three cases separately.

5.1. **Case I-i.** Assume that the polynomial $\hat{p}(y)$ has one simple real root and two complex roots, that is, $\hat{p}(y) = b_5(y-r)(y-(a+ib))(y-(a-ib))$ and the same happens for $\hat{q}(x)$ with roots ρ, and $\alpha \pm i\beta$. It is clear that in this case system (6) has four finite equilibrium points, namely, $e_1 = (0,0)$, $e_2 = (0,r)$, $e_3 = (\rho, 0)$ and $e_4 = (\rho, r)$.

We have that

$$H_2''(y) = \frac{1}{(a^2+b^2)\,r}(4y^3 - 3(2a+r)y^2 + 2\left(a^2+2ra+b^2\right)y - \left(a^2+b^2\right)r),$$

and

$$H_1''(x) = \frac{1}{(\alpha^2+\beta^2)\,\rho}(-4x^3 + 3(2\alpha+\rho)x^2 - 2\left(\alpha^2+2\rho\alpha+\beta^2\right)x + \left(\alpha^2+\beta^2\right)\rho).$$

Thus from the analysis of the linear part at each equilibrium point and using Lemma 3, we obtain that: e_1 is a center, e_2 is a saddle with eigenvalues $\pm\lambda_2$, e_3 is a saddle with eigenvalues $\pm\lambda_3$, and e_4 is a center with eigenvalues $\pm i\lambda_4$, where $\lambda_2 = \sqrt{((a-r)^2+b^2)/(a^2+b^2)}$, $\lambda_3 = \sqrt{((\alpha-\rho)^2+\beta^2)/(\alpha^2+\beta^2)}$, and $\lambda_4 = \lambda_2\lambda_3$.

Note that the infinite equilibrium point in U_1 is $P = \left(\left(\frac{(-r(a^2+b^2))}{((\alpha^2+\beta^2)\rho}\right)^{1/5}, 0\right)$, is a stable node if $r > 0$ and an unstable node if $r < 0$ and the stability of the corresponding equilibrium in V_1 is the opposite.

From the previous analysis we have that system (6) in the case I-i has four finite equilibria, two of them are centers and two are saddles, and has two infinite nodes. So we conclude that the local phase portrait at the equilibria of system (3) for the I-i is the one indicated in Figure 7.

Note that doing the change of variables $(x, y, t, r) \to (x, -y, -t, -r)$ we reverse the orientation of the orbits but it is sufficient to study the case $r > 0$ and doing the change $(x, y, t, \rho) \to (-x, y, -t, -\rho)$ it is sufficient to study the case $\rho > 0$. Moreover, under the composition of these two changes we can consider that $r > 0$ and $\rho > 0$.

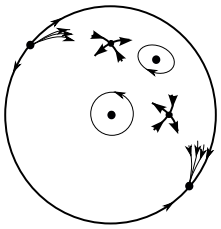

FIGURE 7. Local phase portrait of the equilibria of for the system (3) in the case I-i.

Now we will determine the global phase portraits using the previous information and the connections between the separatrices of the saddles. First we analyze the vector field over the straight lines that contain the finite equilibria $x = 0$, $x = \rho$, $y = 0$ and $y = r$ (assuming $r > 0$ and $\rho > 0$) and we get

$$\dot{x}\begin{cases} > 0 & \text{if } y < 0, \\ < 0 & \text{if } 0 < y < r, \\ > 0 & \text{if } x > r, \end{cases} \quad \text{and } \dot{y}\begin{cases} < 0 & \text{if } x < 0, \\ > 0 & \text{if } 0 < x < \rho, \\ < 0 & \text{if } x > \rho, \end{cases}$$

as it is shown in Figure 8.

This information implies that the stable separatrix of e_2 located in the region $x < 0$ and $y > r$ must connect with the infinite node in V_1, while the unstable separatrix of e_3 in the region $x > \rho$ and $y < 0$ must connect with the stable node in U_1. Furthermore, the unstable separatrix of e_2 (that locally satisfies $y > r$) must cross the straight line $x = \rho$ and after that must cross the straight line $y = r$, the other

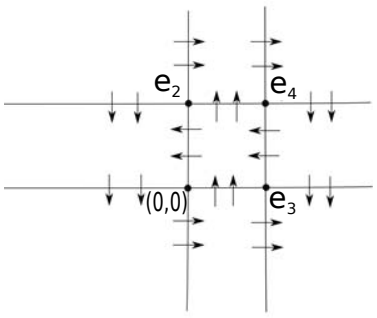

FIGURE 8. Flow of system (3) over the straight lines $x = 0$, $x = \rho$, $y = 0$ and $y = r$ in the case I-i.

unstable separatrix of e_2 cross the straight line $y = 0$ and after that cross the y-axis and pass to the region $x > 0$. But we cannot decide from Figure 8 what is the ω-limit of the unstable separatrices of e_2.

In order to complete all possible connections of separatrices, we are going to take into account the energy levels of the saddle points. The energy levels are $h_2 = H(e_2) = (r^2(10(a^2 + b^2) - 10ar + 3r^2))/(60(a^2 + b^2)) > 0$ and $h_3 = H(e_3) = (\rho^2(10(\alpha^2 + \beta^2) - 10\alpha\rho + 3\rho^2))/(60(\alpha^2 + \beta^2)) > 0$.

Define $\nu_2(y) = -h_2 + H_2(y)$, so as $\nu_2'(y) = H_2'(y)$ and as we know that $H_2'(y)$ has only two different real roots, the function $\nu_2(y)$ must have exactly two roots (one positive at r with multiplicity two and one negative), because $h_2 > 0$ and $b_5 < 0$ (for $r > 0$), as in Figure 9. Thus $H_2(y) = h_2$ intersects twice the y-axis, once in the region $y > 0$ and once in the region $y < 0$. Analogously we consider the auxiliary function $\nu_3(x) = -h_3 + H_1(x)$ which has the same properties than $\nu_2(y)$, so the curve on the energy level $H_1(x) = h_3$ intersects the x-axis once in the region $x < 0$ and once in the region $x > 0$.

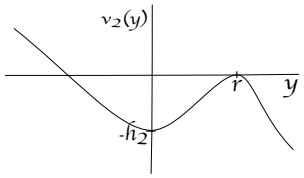

FIGURE 9. The graphic of the auxiliary function $\nu_2(y)$.

Since we are interested in the possible connections between the saddles, we can distinguish three cases, namely, $h_2 = h_3$, $h_2 < h_3$ and $h_3 < h_2$.

If $h_2 = h_3$ and since the energy level $H_2(y) = h_2$ intersects the y-axis exactly twice, it follows that the saddles e_2 and e_3 are connected by their separatrices and they form the boundary of the period annuli of the centers at the origin and at e_4 (see Figure 11(b)). More precisely the two unstable separatrices of e_2 must connect with the two stable separatrices of e_3 surrounding the two centers, and the stable separatrix of e_2 in the region $x > 0$ must connect with the unstable separatrix of e_3 in the region $y > 0$ passing between the two centers. Therefore the global phase portrait is shown in Figure 11(b).

In the case $h_2 < h_3$ since the origin and e_4 are centers, the boundary of their period annuli is formed by a homoclinic loop associated to a saddle, because the infinite equilibrium points are nodes. Furthermore defining $\mu_2(x) = -h_2 + H_1(x)$ and as $\mu_2(0) = -h_2 < 0$, $b_5 < 0$ the graphic of $\mu_2(x)$ cuts once the negative x-axis, and as $\mu_2(\rho) = -h_2 + h_3$ we have that $\mu_2(\rho) > 0$, thus $\mu_2(x)$ cuts twice the positive x-axis ($\rho > 0$)

as in shown in Figure 10(a). Thus considering the previous analysis and the information given by the study of ν_2 and ν_3 we can conclude that the separatrices of the saddle e_2 located in region $y < r$ form the boundary of the period annulus of the origin, and their unstable separatrix in $y > r$ must connect with the infinite equilibrium in U_1. Following the same previous argument, we have that the boundary of the period annulus of e_4 is formed by a homoclinic loop of the stable and unstable separatrices of e_3 that are located in the first quadrant (see Figure 11(a)), the remaining stable separatrix of e_3 located in the fourth quadrant must connect with the infinite equilibrium point in V_1. These information force that the global phase portrait in this case is topologically equivalent to the one shown in Figure 11(a).

Finally in the case $h_2 > h_3$ the analysis is quite similar to the previous case. Here, $\mu_2(\rho) < 0$, so the auxiliary function $\mu_2(x)$ does not have positive roots (see Figure 10(b)), this implies that the energy level $H_2(y) = h_2$ intersect only once the x-axis and for a negative value. These forces that the unstable separatrix of e_2 in $y < r$ must connect with the infinite equilibrium P, and therefore the boundary of the period annulus of the center at the origin is formed by separatrices of e_3 located in the region $x < \rho$. The behavior of the vector field on the axes described in Figure 8 implies that the center e_4 is in an annular region whose boundary is formed by separatrices of e_2 located in the first quadrant (see Figure 11(c)). By continuity we can complete the connections associated to the remaining stable separatrix of e_3, as do not exist more finite equilibria, they must connect with the infinite equilibrium in V_1.

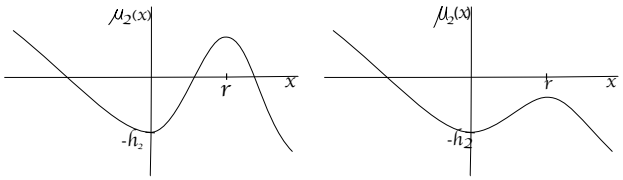

FIGURE 10. The graphic of the auxiliary function $\mu_2(x)$. (a) $h_2 < h_3$. (b) $h_2 > h_3$.

The previous analysis shows that the global phase portrait in this case is topologically equivalent to the one shown in Figure 11(c). Therefore we have concluded the proof in the case I-i.

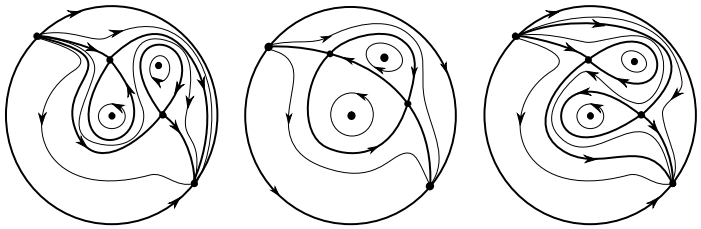

FIGURE 11. Phase portraits for the systems associated to the Hamiltonian (5) when the roots of $\hat{p}(y)$ are $r \in \mathbb{R}$ and $a \pm ib$, and the roots of $\hat{q}(x)$ are ρ and $\alpha \pm i\beta$. The separatrices are in bold. (a) $h_2 < h_3$. (b) $h_2 = h_3$. (c) $h_2 > h_3$.

5.2. **Case I-iii.** Assuming that $\hat{p}(y) = b_5(y-r)(y-(a+ib))(y-(a-ib))$ and the polynomial $\hat{q}(x)$ has one root ρ of multiplicity three (triple root). The Hamiltonian system given in (6) becomes

$$\dot{x} = \frac{1}{r\,(a^2+b^2)} y(y-r)\left((y-a)^2+b^2\right), \quad \dot{y} = -\frac{1}{\rho^3} x(x-\rho)^3. \tag{18}$$

System (18) has four finite equilibria, the center at the origin, $e_2 = (\rho, 0)$, $e_3 = (0, r)$ and $e_4 = (\rho, r)$. The equilibrium e_3 is a saddle with eigenvalues $\lambda = \pm\sqrt{((a-r)^2+b^2)/(a^2+b^2)}$, e_2 and e_4 are both nilpotent, where by Lemma 4 e_2 is a saddle because $f_2(0) > 0$, and e_4 is a center because $f_2(r) < 0$.

At the infinite region the equilibrium P is a stable node if $r > 0$ and an unstable node if $r < 0$.

From the previous information we have that the local phase portrait of system (18) is as in Figure 7.

As in the case I-i it is sufficient to study the case $r, \rho > 0$ because of symmetries $(x, \rho, t) \to (-x, -\rho, -t)$, $(y, r, t) \to (-y, -r - t)$ and $(x, y, \rho, r) \to (-x, -y, -\rho, -r)$. On the other hand we observe that the local phase portrait of both cases I-i and I-iii are the same. Using the same arguments as in the case I-i, but taken the level of energy of the finite saddle $h_2 = H(\rho, 0) = \rho^2/20$ and $h_3 = H(0, r) = h_3 = (r^2\left(10\left(a^2+b^2\right) - 10ar + 3r^2\right))/(60\left(a^2+b^2\right))$, we obtain that the global phase portraits of system (18) are topologically equivalent to the ones of Figure 11.

5.3. **Case III-iii.** Now we consider the case where the polynomials $\hat{p}(y)$ and $\hat{q}(x)$ have one triple real root r and ρ, respectively. In this case system (3) takes the form

$$\dot{x} = \frac{1}{r^3} y(y-r)^3, \quad \dot{y} = -\frac{1}{\rho^3} x(x-\rho)^3. \tag{19}$$

In order to characterize the local phase portrait, we first study the finite equilibria which are: the center at the origin, $e_2 = (0, r)$ and $e_3 = (\rho, 0)$ which are nilpotent and $e_4 = (\rho, r)$ which is degenerate. Applying Lemma 4 we obtain that both nilpotent equilibria are saddles because $f_1(0) > 0$ and $f_2(0) > 0$. By Lemma 5 we get that e_4 is a center.

On the other hand in this case the infinite equilibrium is a stable node if $r > 0$ and an unstable node if $r < 0$.

From the previous analysis we obtain that the local phase portrait of system (19) is as in Figure 7, in particular the local phase portrait in this case coincides with the cases I-i (or I-iii).

Defining the level of energy of the finite saddles by $h_2 = H(0, r) = r^2/20$ and $h_3 = H(\rho, 0) = \rho^2/20$, and taking into account that the local phase portrait agree with case I-i, we get that the global phase portrait in this case is topologically equivalent to Figure 11(a) if $r^2 < \rho^2$, to Figure 11(b) if $r^2 = \rho^2$ and to Figure 11(c) if $r^2 > \rho^2$. Thus we have completed the proof of statement (a) of Theorem 1.

6. Proof of Theorem 1 statement (b)

In this case the polynomial $\hat{p}(y)$ (respectively $\hat{q}(x)$) has one real root with multiplicity three or one real and two complex, and the polynomial $\hat{q}(x)$ (respectively $\hat{p}(y)$) has two real roots one of them of multiplicity two. In order to get the proof of this statement, according to Remark 2 it is sufficient to study only the cases I-ii and II-iii.

6.1. **Case I-ii.** Here $\hat{q}(x)$ has real roots ρ and σ, where σ has multiplicity two (double root) and $\hat{p}(y)$ has one real root r and two complex roots $a \pm ib$. In this situation system (6) is written as

$$\dot{x} = \frac{1}{r\left(a^2+b^2\right)} y(y-r)\left((y-a)^2+b^2\right), \quad \dot{y} = -\frac{1}{\rho\sigma^2} x(x-\rho)(x-\sigma)^2. \tag{20}$$

It is clear that system (20) has five finite equilibrium points besides the origin, namely: $e_2 = (\sigma, 0)$, $e_3 = (\rho, 0)$, $e_4 = (0, r)$, $e_5 = (\sigma, r)$ and $e_6 = (\rho, r)$. According to Lemma 3 it is verified that the hyperbolic equilibria e_3 and e_4 are saddles, whose associated eigenvalues are $\lambda = \pm(1 - \rho/\sigma)$, and $\lambda = \pm\sqrt{(b^2 + (a-r)^2)/(a^2+b^2)}$, respectively. The equilibrium e_6 is a center whose associated eigenvalues are $\lambda = \pm i((\rho-\sigma)/\sigma)\sqrt{(b^2+(a-r)^2)/(a^2+b^2)}$. By Lemma 4 the equilibria e_2 and e_5 are nilpotent and

are cusps. Even more, the local phase portraits of e_2 and e_5 are shown in Figure 12. This completes the local phase portraits in the finite region.

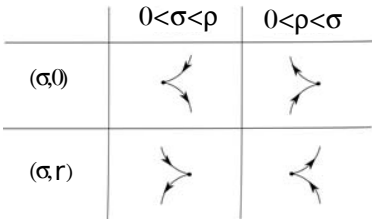

FIGURE 12. Local phase portraits of the cusp $e_2 = (\sigma, 0)$ and $e_5 = (\sigma, r)$ of system (20) according sign of $\sigma - \rho$ (assuming $\sigma, \rho > 0$).

At infinity the infinite equilibrium point P is a stable node if $r > 0$ and it is an unstable node if $r < 0$.

In order to describe the local and global phase portraits we observe that it is sufficient to analyze the cases $r > 0$ and $0 < \rho < \sigma$, and $r > 0$ and $0 < \sigma < \rho$. In fact system (20) possesses the reverse symmetry: $y \to -y$, $t \to -t$, $r \to -r$ which allows to assume $r > 0$. The other situation follows considering the change of variables $(x, y) \mapsto (x - \rho, -y + r)$ which allows to study only the case $\rho > 0$, and the change of variables $(x, y) \mapsto (-x + \rho, -y + r)$ permit us to consider only the situation $\sigma > 0$. Finally using the time reversing symmetry $x \to -x$, $t \to -t$, $\rho \to -\rho$, $\sigma \to -\sigma$ it is sufficient to study the cases when $\rho > 0$ and $\sigma > 0$ simultaneously, that is, we need to study the cases: $r > 0$ and $0 < \rho < \sigma$, and $r > 0$ and $0 < \sigma < \rho$. Therefore we summarize in Figure 13 the local phase portraits on the Poincaré disc, according the sign of $\sigma - \rho$.

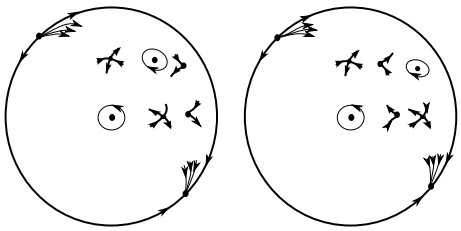

FIGURE 13. Local phase portraits at the equilibria of system (3) in the case I-ii for $r > 0$. (a) $0 < \rho < \sigma$. (b) $0 < \sigma < \rho$.

Now we are going to determine all possible global phase portraits for the case $r > 0$ and $0 < \rho < \sigma$ and for the case $r > 0$ and $0 < \sigma < \rho$. First we point out some properties of the Hamiltonian vector field on the axes:

$$\dot{x} \begin{cases} > 0 & \text{if } y < 0, \\ < 0 & \text{if } 0 < y < r, \\ > 0 & \text{if } x > r, \end{cases}$$

and

$$\dot{y} \begin{cases} < 0 & \text{if } x < 0, \\ > 0 & \text{if } 0 < x < \rho, \\ < 0 & \text{if } \rho < x < \sigma, \\ < 0 & \text{if } x > \sigma, \end{cases} \quad \text{and} \quad \dot{y} \begin{cases} < 0 & \text{if } x < 0, \\ > 0 & \text{if } 0 < x < \sigma, \\ > 0 & \text{if } \sigma < x < \rho, \\ < 0 & \text{if } x > \rho. \end{cases}$$

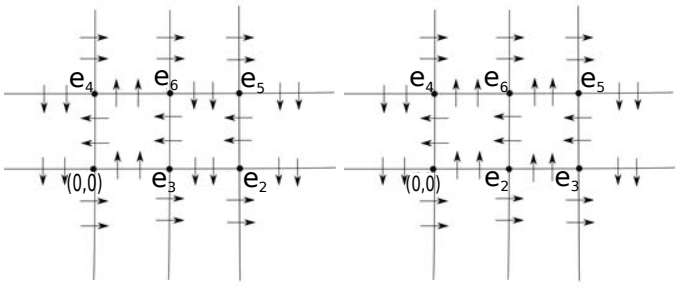

(a) (b)

FIGURE 14. Flow of the vector field (3) over the straight lines $x = 0$, $x = \rho$, $x = \sigma$, $y = 0$ and $y = r$ in the case I-ii. (a) $0 < \rho < \sigma$. (b) $0 < \sigma < \rho$.

There behaviors are shown in Figure 14.

In order to establish the possible connections between the separatrices of the finite and infinite equilibria, in addition to the above information, we must analyze the energy levels of the finite equilibria (associated to the saddles and cusps) $h_i = H(e_i)$ which are $h_2 = (5\rho - 2\sigma)\sigma^2/(60\rho)$, $h_3 = \rho^2(3\rho^2 - 10\rho\sigma + 10\sigma^2)/(60\sigma^2)$, $h_4 = r^2(10(a^2 + b^2) - 10ar + 3r^2)/(60(a^2 + b^2))$ and $h_5 = h_2 + h_4$.

First we study the case $0 < \rho < \sigma$ and $r > 0$. From Figure 14(a) it easily follows that the stable separatrix of e_4 located in the region $\{(x, y) : x < 0, y > r\}$ cannot go to out of this region, so it must connect with the unstable node in V_1. Similarly the unstable separatrix of the cusp e_2 must connect with the infinite stable node located at U_1. Also the unstable separatrix of e_3 in the region $x > \rho$, $y < 0$ must connect with the same infinite node in U_1 (see Figure 17). Again using the analysis given by Figure 14(a) we observe that the unstable separatrix of e_4 with $x > 0$ must cross the straight line $x = \sigma$ with $y > r$, the other unstable separatrix of e_4 must first cross the straight line $x = 0$ with $y < 0$ and after that it cuts the y-axis with $y < 0$ (see Figure 15(a)). On the other hand for the cusp e_5 we can only affirm that its stable separatrix cuts (in backward time) the straight line $x = \sigma$ with $y > r$. In addition the stable separatrix of the saddle e_3 in region $y < 0$ cuts the x-axis with $y < 0$ (in backward time). Finally we can say that for the cusp e_2 the unstable separatrix cuts (in backward time) the straight line $y = r$ with $x > \rho$ and previously it cuts the straight line $x = \sigma$ with $y > r$ (see Figure 17). However with the analysis of the vector field on the straights lines containing the equilibria, we cannot conclude who are the α and ω limits of all the separatrices, but we are able to complete the global phase portraits using the relations of the energy levels h_i, as we have done in the proof of statement (a) of Theorem 1.

Since, e_1 and e_6 are centers, we need to do a complete analysis, in the subcases $h_i \le h_j \le h_k \le h_l$, for the energy levels h_2, h_3, h_4 and h_5.

In this case we have that $h_2 < h_5$ and $h_2 < h_3$, and then there exist 18 possible relations between the energy level of the saddles and cusps: (a) $h_2 < h_3 = h_4 = h_5$, (b) $h_2 = h_4 < h_3 = h_5$, (c) $h_2 = h_4 < h_5 < h_3$, (d) $h_2 < h_4 = h_5 < h_3$, (e) $h_2 < h_3 < h_4 < h_5$, (f) $h_2 < h_3 < h_4 = h_5$, (g) $h_2 < h_3 < h_5 < h_4$, (h) $h_2 < h_3 = h_4 < h_5$, (i) $h_2 < h_4 < h_3 < h_5$, (j) $h_2 < h_4 < h_3 = h_5$, (k) $h_2 < h_4 < h_5 < h_3$, (l) $h_2 < h_3 = h_5 < h_4$, (m) $h_4 < h_2 < h_3 < h_5$, (n) $h_4 < h_2 < h_3 = h_5$, (o) $h_4 < h_2 < h_5 < h_3$, (p) $h_2 < h_5 < h_3 < h_4$, (q) $h_2 < h_5 < h_3 = h_4$ and (r) $h_2 < h_5 < h_4 < h_3$. Next we give a complete study of the global phase portrait for four representative cases of the 18. The analysis in the remaining cases is similar.

Analysis of the case (a) $h_2 < h_3 = h_4 = h_5$. Previously we observe that the unstable separatrix of e_4 with $x > 0$ must cross the straights line $x = \sigma$ with $y > r$, in this case we can affirm that this

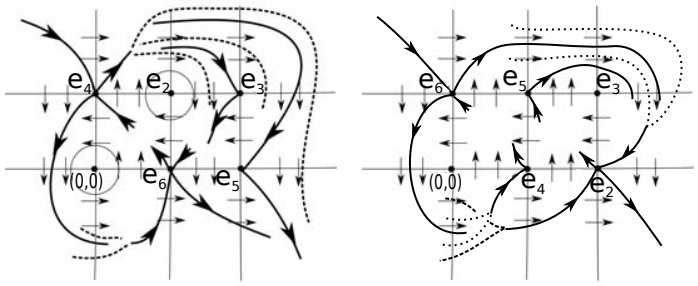

(a) (b)

FIGURE 15. Phase portraits of separatrices in system (3) in the case I-ii with $r > 0$. (a) $0 < \rho < \sigma$. (b) $0 < \sigma < \rho$

separatrix must connect with the stable separatrix of the cusp e_5, because as $h_2 < h_3$ it cannot connect with the stable separatrix of e_2 and it cannot connect with the stable node in U_1 because the roots of the polynomial $H_1(x) - h_3$ are two, one for $x < 0$ and other in $x = \rho$. Using these informations we obtain that the stable separatrix of the saddle e_4 in the region $x > 0$ must connect with the unstable separatrix of e_3 with $y > 0$, and the unstable separatrix of e_5 must connect with the stable separatrix of the saddle e_3 in the region $x > 0$. Thus these three last connections form the boundary of the period annulus of the center e_6. Also it follows that the unstable separatrix of e_4 (with $y < r$) and the stable separatrix of e_3 in the region $y < 0$ are connected forming the boundary of the period annulus of the center at the origin. Finally by continuity it follows that the unstable separatrix of e_2 in $x > 0$ must connect with the unstable node of the chart V_1. Therefore the global phase portrait for the case (a) is shown in Figure 16(a).

Analysis of the case (b) $h_2 = h_4 < h_3 = h_5$. Again we remember that previously the unstable separatrix of e_4 with $x > 0$ must cross the straight line $x = \sigma$ with $y > r$, here we can affirm that this separatrix must connect with the stable separatrix of the cusp e_2, because as $h_4 < h_5$ it cannot connect with the stable separatrix of e_5 and it cannot connect with the stable node in U_1 because the roots of polynomial $H_1(x) - h_2$ are three, one for $x < 0$, one in $0 < x < \rho$ and in $x = \sigma$. Moreover the above arguments imply that the separatrices of the saddle e_4 in the region $y < r$ form the boundary of the period annulus of the origin. By continuity it follows that the stable separatrix of e_3 in $y < 0$ must connect with the unstable node of the chart V_1. Using the same type of arguments and since $h_3 = h_5$, we get that the separatrices of e_3 (with $y > 0$) and the separatrices of e_5 are connected forming the boundary of the period annulus of the center e_6. Therefore the global phase portrait for the case (b) is described in Figure 16(b).

Analysis of the case (c) $h_2 = h_4 < h_5 < h_3$. In this case for the unstable separatrix of e_4 with $x > 0$ that cross the straight line $x = \sigma$ with $y > r$ we can follow the analysis of the case (b), and as $h_2 = h_4$ must connect with the stable separatrix of the cusp e_2, because since $h_4 < h_5$ it cannot connect with the stable separatrix of e_5 and it cannot connect with the stable node in U_1 because the polynomial $H_1(x) - h_2$ has three roots, one for $x < 0$, one in $0 < x < \rho$ and in $x = \sigma$. In addition using the above arguments the energy level h_2 implies that the separatrices of the saddle e_4 in the region $y < r$ form the boundary of the period annuli of the origin as in the case (b). On the other hand the polynomial $H_1(x) = h_5$ has one negative root and two positive roots (one in $0 < x < \rho$ ans the other in $x > \sigma$), thus the energy level $H = h_5$ cuts three times the x-axis, this implies that the unstable separatrix of e_5 must connect with the infinite node in U_1, and the stable separatrix cuts the x-axis in the region $0 < x < \rho$ and another time in the region $x < 0$. This information and since the polynomial $H_2(y) - h_3$ does not has

positive roots forces that the separatrices of the saddle e_3 in the region $y > 0$ form the period annulus of the center e_6. Then by continuity we can conclude that the stable separatrix of e_3 in $y < 0$ must connect with the unstable node of the chart V_1. The above analysis allows conclude that the global phase portrait for the case (c) is shown in Figure 16(c).

Now we analyze one case where all the saddles and cusps have different energy levels. As an example, we consider the case (e) $h_2 < h_3 < h_4 < h_5$. Considering the energy level $H = h_3$ we must pay attention to the fact that the curve $H_2(y) = h_3$ intersects three times the y-axis, in the region $y < 0$, in $0 < y < r$ and in $y > r$. Also we observe that the polynomial $H_1(x) - h_3$ only has two roots, in the region $x < 0$ and in $x = \rho$ (which is a maximum), thus the two separatrices of e_3 in the region $x < \rho$ form a homoclinic loop surrounding the period annulus of the center at the origin (we need more information to conclude the trajectory of the stable separatrix of e_3 in the region $x > \rho$). On the other hand the polynomial $H_1(x) - h_5$ does not has roots and the polynomial $H_2(y) - h_5$ neither has roots, so the energy level $H = h_5$ does not cross the axes, this implies that the separatrices of the cusp e_5 form a homoclinic loop that encloses the period annulus of the center e_6.

Now we characterize the trajectories of the remaining separatrices of e_4 (remember that the stable separatrix in the region $x < 0$ must connect with the node in V_1). We observe that $H_1(x) = h_4$ has only a negative zero (it does not have positive zeros) and for the study that was carried out above we know that the unstable separatrix in region $x < 0$ crosses the x-axis, so the other two separatrices of e_4 are connected forming a homoclinic orbit, by continuity this contains the homoclinic loop of the separatrices of e_5. Finally by continuity we can conclude that the unstable separatrix of e_4 that crosses the x-axis must connect with the infinite stable node in U_1. The stable separatrix of e_3 in the region $x > \rho$ crosses the straight line $y = r$ with $x > \sigma$ and then must connect with the infinite unstable node in V_1. Similarly the stable separatrix of the cusp e_2 must connect with the infinite unstable node in V_1. Thus the previous analysis provides the global phase portrait of the case (e) and this is the one shown in Figure 16(e).

The global phase portraits for the remaining 14 cases are shown in Figure 16. The proof of the global phase portraits on the Poincaré disc follows the same types of arguments that we have used for the cases (a), (b), (c) and (e). By this reason, we omit the details of the analysis for the other cases.

Now we are going to study the case $0 < \sigma < \rho$ and $r > 0$. Note that the location of the finite equilibria on the Poincaré disc differs of the previous cases, this is a first difference. Next we point out that due to the inequalities of the roots, it is verified that $h_5 > h_2$, $h_5 > h_4$ and $h_3 > h_2$. Therefore there are 11 possible relations between the energy levels given by: (a) $h_2 = h_4 < h_3 = h_5$, (b) $h_2 = h_4 < h_3 < h_5$, (c) $h_2 = h_4 < h_5 < h_3$, (d) $h_2 < h_3 < h_4 < h_5$, (e) $h_2 < h_3 = h_4 < h_5$, (f) $h_2 < h_4 < h_3 < h_5$, (g) $h_2 < h_4 < h_3 = h_5$, (h) $h_2 < h_4 < h_5 < h_3$, (i) $h_4 < h_2 < h_3 < h_5$, (j) $h_2 < h_4 < h_3 = h_5$ and (k) $h_4 < h_2 < h_5 < h_3$. Thus the description of all the possible global phase portraits is reduced to the study of these 11 cases. Note that in this situation, unlike of the first case, we do not have the possibilities that three energy levels be equal. In order to obtain the global phase portrait, we use the same ideas than in the first case (when $0 < \rho < \sigma$ and $r > 0$). In fact we need to determine all the possible connections between the separatrices, as we know that they depend on the energy levels. Initially we deliver some results independent of the energy for the phase portrait of separatrices associated to saddles and cusps. As in the first case ($0 < \rho < \sigma$ and $r > 0$), the stable separatrix of e_4 in the region $y > r$ and $x < 0$ cannot go out of this region and then it must connect with the infinite node in V_1 (see Figure 17). The unstable separatrix of the saddle e_3 in the region $x > \rho$ must connect with the infinite node in U_1 according to Figure 14(b). Also the stable separatrix of e_3 located in this region cuts the straight line $y = r$ with $x > \rho$ and after that cuts (in backward time) the straight line $x = \rho$ with $y > r$. The other stable separatrix of e_3 (in $x < \rho$) must cross the straights lines $x = \sigma$ and $x = 0$ with $y < 0$, and after that (in backward time) cuts the x-axis with $x < 0$, see Figure 15(b). On the other hand the unstable separatrix of e_4 in the region $y > r$ must cut the straight line $x = \rho$ and then must cut the straight line $x = \sigma$. Moreover after that the separatrix cuts the straight line $y = r$ with $x > \rho$. The other unstable separatrix of e_4 in

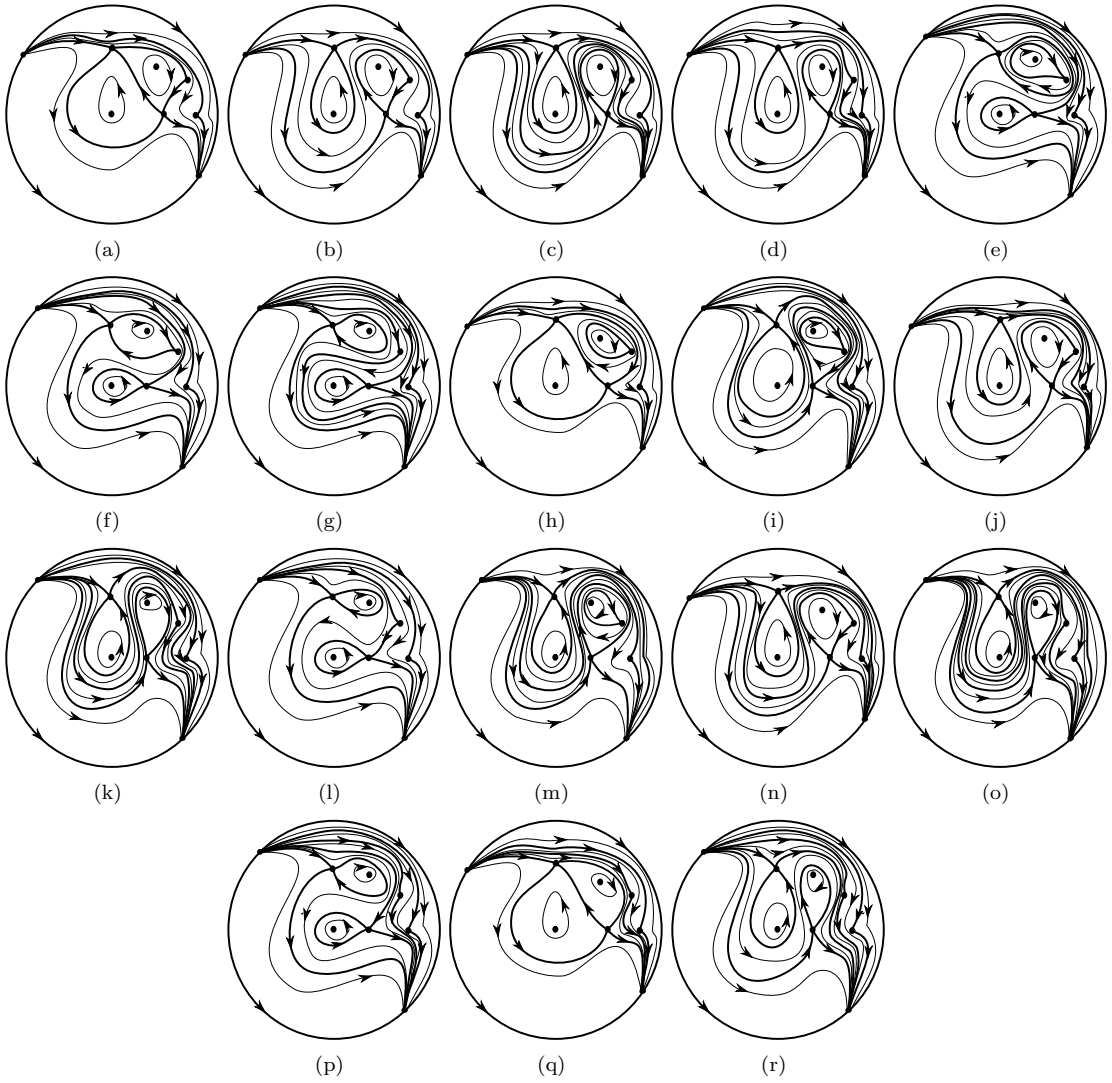

FIGURE 16. Global phase portraits for the system (3) in the case I-ii for $r > 0$ and $0 < \rho < \sigma$. (a) $h_2 < h_3 = h_4 = h_5$. (b) $h_2 = h_4 < h_3 = h_5$. (c) $h_2 = h_4 < h_5 < h_3$. (d) $h_2 < h_4 = h_5 < h_3$. (e) $h_2 < h_3 < h_4 < h_5$. (f) $h_2 < h_3 < h_4 = h_5$. (g) $h_2 < h_3 < h_5 < h_4$. (h) $h_2 < h_3 = h_4 < h_5$. (i) $h_2 < h_4 < h_3 < h_5$. (j) $h_2 < h_4 < h_3 = h_5$. (k) $h_2 < h_4 < h_5 < h_3$. (l) $h_2 < h_3 = h_5 < h_4$. (m) $h_4 < h_2 < h_3 < h_5$. (n) $h_4 < h_2 < h_3 = h_5$. (o) $h_4 < h_2 < h_5 < h_3$. (p) $h_2 < h_5 < h_3 < h_4$. (q) $h_2 < h_5 < h_3 = h_4$. (r) $h_2 < h_5 < h_4 < h_3$.

the region $x < 0$ and $y < r$ must cut the x-axis with $x < 0$, and then must cut the y-axis with $x < 0$. For the cusp e_2 we only can affirm that its stable separatrix must cut the y-axis with $x < 0$.

Finally as general behavior we note that the unstable separatrix of the cusp e_5 necessarily cuts the line $x = \rho$ with $y > r$ and after that cuts the straight line $y = r$ with $x > \rho$ (this information is summarized in Figure 15(b)).

It is clear from the previous analysis that we cannot conclude which are the α and ω limits of all the separatrices. As in the case $0 < \rho < \sigma$, we are going to complete the global phase portrait using the relations between the energy levels h_i, which allows to determine all the possible connections.

Since the procedure to describe the global phase portrait in each of the 11 cases mentioned is similar to the case $0 < \rho < \sigma$, we do a complete analysis only in two of these cases.

Analysis of the case (a): $h_2 = h_4 < h_3 = h_5$. Here the saddle e_4 and the cusp e_2 are in the same energy level and as the polynomial $H_1(x) - h_2$ has three zeros: in $x < 0$, at $x = \sigma$ and in $x > \rho$, we obtain that the separatrices of the cusp e_2 must connect with the two separatrices of e_4 located in the region $y < r$ forming the boundary of the period annulus of the center at the origin (see Figure 17(a)). Even more the unstable separatrix of e_4 in $y > r$ that cross the straight line $x = \sigma$ must crosses the straight line $y = r$ in $x > \rho$, implying that this separatrix must connect with the infinite node in U_1, thus we have already characterized all the separatrices of e_4 and e_2. On the other hand the polynomial $H_1(x) - h_3$ only has one positive root x-axis at $x = \rho$, and a negative root in $x < 0$. This implies that the separatrices of the cusp e_3 must connect with the separatrices of the saddle e_5 in the region $y > 0$, so these connections surround the period annulus of the center e_6. Lastly from the previous fact and by continuity the stable separatrix of e_3 in $y < 0$ after crossing the x-axis in $x < 0$ must connect with the infinite unstable node in V_1. From the previous analysis we conclude that in this case the global phase portrait is as the one of Figure 17(a).

Analysis of the case (d): $h_2 = h_4 < h_3 = h_5$. Initially we characterize the separatrices of the cusps e_2 and e_5. As the polynomial $H_1(x) - h_2$ have two roots, in $x < 0$ and in $x = \sigma$, and in addition the polynomial $H_2(y) - h_2$ has one root in $y < 0$ and one in $0 < y < r$, we have that the separatrices of e_2 must connect together forming the boundary of the period annulus of the center at the origin. On the other hand the polynomial $H_1(x) - h_5$ does not has positive roots, and the polynomial $H_2(y) - h_5$ has no positive roots, these imply that the separatrices of the cusp e_5 form a homoclinic loop enclosing the period annulus of the center e_6. In relation to the energy level of the saddle e_3 we obtain that the polynomial $H_1(x) - h_3$ has two roots, one in $x < 0$ and the other at $x = \rho$, and the polynomial $H_2(y) - h_3$ has three roots, in $y < 0$, in $0 < y < r$ and in $y > r$. The previous sentences imply that the separatrices of e_3 in the region $x < \rho$ must connect together enclosing the homoclinic loop formed by the separatrices of e_2. Furthermore the stable separatrix of this saddle e_4 that crosses the straights lines $y = r$, $x = \rho$ and $x = \sigma$ must connect with the infinite node in V_1. Finally using the continuity of the flow and following the previous reasoning we obtain that the separatrices of e_4 in the region $x > 0$ are connected surrounding the homoclinic loop formed by the separatrices of the cusp e_5, and the unstable separatrix of this saddle e_4 that crosses the y-axis with $y < 0$ must connect with the infinite node in U_1. The above analysis and the results given previously allows to conclude that the global phase portrait in this case is the one shown in Figure 17(d).

The global phase portraits for the remaining 9 cases are shown in Figure 17.

Thus we have concluded the study of the global phase portraits in the case I-ii.

6.2. **Case II-iii.** Suppose now that the polynomial $\hat{q}(x)$ has one triple real root ρ and $\hat{p}(y)$ has real roots r and s, with s a double root. Thus system (6) is equivalent to

$$\dot{x} = -\frac{1}{rs^2} y(r-y)(s-y)^2, \quad \dot{y} = -\frac{1}{\rho^3} x(x-\rho)^3. \tag{21}$$

There exist six finite equilibria, namely, $e_1 = (0,0)$, $e_2 = (0,r)$, $e_3 = (0,s)$, $e_4 = (\rho,0)$, $e_5 = (\rho,r)$ and $e_6 = (\rho,s)$. The origin is a center as we know, e_2 is a saddle with eigenvalues $\pm(1 - r/s)$. The other four equilibria are not hyperbolic, three of them (e_3, e_4 and e_5) are nilpotent and e_6 is degenerate. As s is a double root of $H_2'(y)$, by Lemma 4 we can conclude that e_3 is a cusp. On the other hand ρ is a triple root of $H_1'(x)$, thus the nilpotent equilibria e_4 and e_5 can be a saddle or a center. Following the statements of

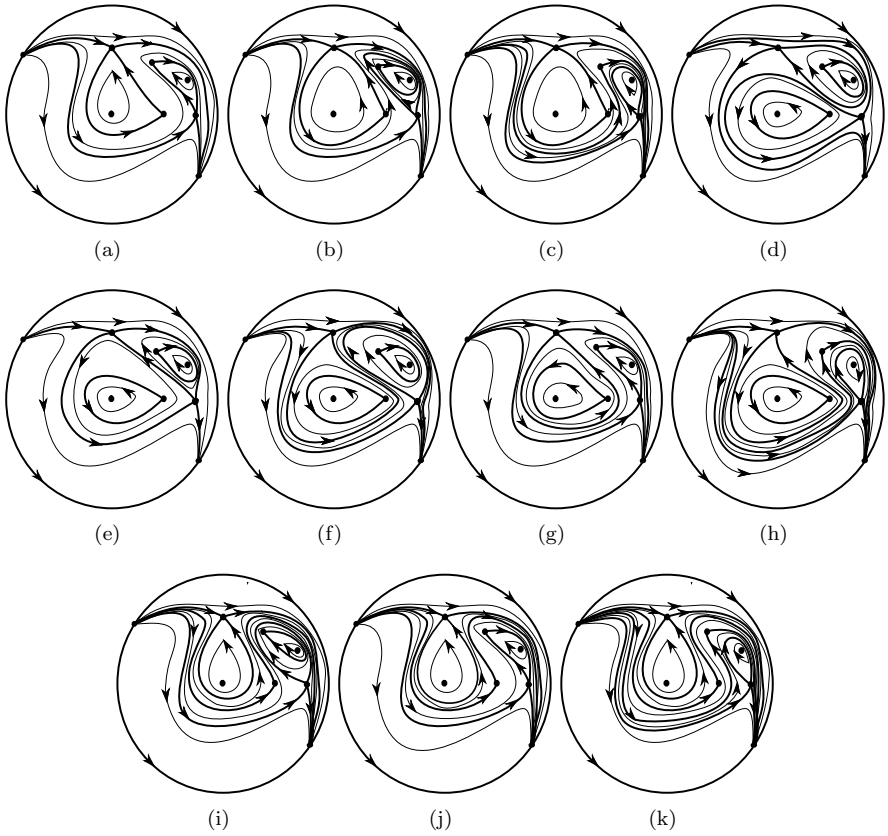

FIGURE 17. Global phase portraits for the system (3) in the case I-ii for $r > 0$ and $0 < \sigma < \rho$. (a) $h_2 = h_4$ and $h_3 = h_5$. (b) $h_2 = h_4$ and $h_3 < h_5$. (c) $h_2 = h_4$ and $h_5 < h_3$. (d) $h_2 < h_3 < h_4 < h_5$. (e) $h_3 = h_4$ and $h_2 < h_5$. (f) $h_2 < h_4 < h_3 < h_5$. (g) $h_3 = h_5$ and $h_2 < h_4$. (h) $h_2 < h_4 < h_5 < h_3$. (i) $h_4 < h_2 < h_3 < h_5$. (j) $h_3 = h_5$ and $h_2 > h_4$. (k) $h_4 < h_2 < h_5 < h_3$.

Lemma 4 we verify that for e_4 it holds that $f_2(0) > 0$ so it is a saddle, and for e_5 it holds that $f_2(r) < 0$ so it is a center. Since ρ is a triple root of $H_1'(x)$ and r is a double root of $H_2'(y)$, by Lemma 5 it follows that e_6 is a cusp. More precisely, the local phase portrait of e_6 is as Figure 18(a) if $(r-s)/(rs) > 0$, or as Figure 18(b) if $(r-s)/(rs) < 0$. We have obtained the local phase portrait of the finite equilibrium points of the vector field (21).

The infinite equilibria P is a stable node if $r > 0$, and it is an unstable node if $r < 0$. Using the symmetries considered for the case I-ii we can analogously reduce the study of the local phase portraits, considering the location of the equilibria to two cases $\rho > 0$ with $0 < r < s$, or with $0 < s < r$. The local phase portraits of all the equilibrium points are shown in the Poincaré disc in Figure 19.

Note that the local phase portrait is topologically equivalent to the local phase portrait in case I-ii, under the change of variables $(x, y) \mapsto (y, x)$. So the analysis of the global phase portrait follow the same arguments used in the previous case I-ii, considering that now the level of energy of the finite equilibria $h_i = H(e_i)$ are: $h_2 = r^2(3r^2 - 10rs + 10s^2)/(60s^2)$, $h_3 = (5r - 2s)s^2/(60r)$, $h_4 = \rho^2/20$, and $h_5 = h_2 + h_4$,

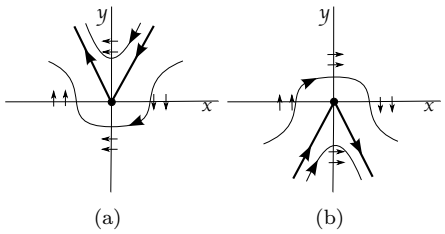

FIGURE 18. Local phase portrait at the equilibrium e_6 of system (21) after translate it to the origin. (a) $(r-s)/(rs) > 0$. (b) $(r-s)/(rs) < 0$.

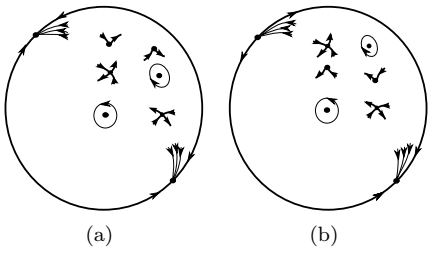

FIGURE 19. Local phase portraits at the equilibria of system 21 in the case II-iii with $\rho > 0$. (a) if $0 < r < s$. (b) if $0 < s < r$.

$h_6 = h_3 + h_4$. Thus the global phase portraits for system (21) are topologically equivalent to one of Figure 16 if $0 < s < r$, or of Figure 17 if $0 < r < s$.

7. Proof of Theorem 1 statement (c)

We consider that $\hat{p}(y)$ (respectively $\hat{q}(x)$) has one real root with multiplicity three or one real and two complex and $\hat{q}(x)$ (respectively $\hat{p}(y)$) have three different real roots, according to Remark 2 it is sufficient to study the cases I-iv and III-iv.

7.1. **Case I-iv.** Considering that the three different real roots of $\hat{q}(x)$ are ρ, σ and τ, and the real root of $\hat{p}(y)$ is r and their complex roots are $a \pm ib$, the associated Hamiltonian system is

$$\dot{x} = -\frac{1}{r\,(a^2+b^2)} y(r-y)\left((a-y)^2+b^2\right), \quad \dot{y} = -\frac{1}{\rho\sigma\tau} x(x-\rho)(x-\sigma)(x-\tau) \tag{22}$$

First we analyze the phase portrait in the finite region. System (22) has eight finite equilibria: The center at the origin, namely e_1, $e_2 = (\rho, 0)$, $e_3 = (\sigma, 0)$, $e_4 = (\tau, 0)$, $e_5 = (0, r)$, $e_6 = (\rho, r)$, $e_7 = (\sigma, r)$ and $e_8 = (\tau, r)$. Next we give the local phase portrait of these equilibrium points. We have by Lemma 3 that $e_5 = (0, r)$ is a saddle with eigenvalues

$$\lambda = \pm\sqrt{(b^2 + (a-r)^2)/(a^2+b^2)}.$$

Furthermore we have three pairs of equilibria formed by one saddle and one center located on a straight line $x = x*$. These are $e_2 = (\rho, 0)$ and $e_6 = (\rho, r)$ whose eigenvalues are

$$\pm\frac{\sqrt{(\rho-\sigma)(\rho-\tau)}}{\sqrt{\sigma}\sqrt{\tau}} \text{ and } \pm\frac{\sqrt{(a^2+b^2)\left((a-r)^2+b^2\right)}}{(a^2+b^2)}\frac{\sqrt{-(\rho-\sigma)(\rho-\tau)}}{\sqrt{\sigma}\sqrt{\tau}},$$

respectively. Another pair is formed for the equilibria $e_3 = (\sigma, 0)$ and $e_7 = (\sigma, r)$ with eigenvalues

$$\pm\sqrt{\frac{-(\rho-\sigma)(\sigma-\tau)}{\rho\tau}} \text{ and } \pm\frac{\sqrt{(a^2+b^2)\left((a-r)^2+b^2\right)}}{(a^2+b^2)}\sqrt{\frac{(\rho-\sigma)(\sigma-\tau)}{\rho\tau}},$$

respectively. The last pair of saddle and center is given by $e_4 = (\tau, 0)$ and $e_8 = (\tau, r)$, these have eigenvalues

$$\pm\sqrt{\frac{(\rho-\tau)(\sigma-\tau)}{\rho\sigma}} \text{ and } \pm\frac{\sqrt{(a^2+b^2)\left((a-r)^2+b^2\right)}}{(a^2+b^2)}\sqrt{\frac{-(\rho-\tau)(\sigma-\tau)}{\rho\sigma}},$$

respectively. Note that on the straight line $y = 0$ there is always two saddles and two centers, this implies that the same happens for the finite equilibria on $y = r$. Furthermore the positions of these saddles and centers are interchanged on these straights lines. From the study of the infinite equilibria we know that in the local chart U_1 there exits a unique equilibria $P = (((-a^2r - b^2r)/(\rho\sigma\tau))^{1/5}, 0)$, by the results in section 4, it is a stable node if $r > 0$ and an unstable node if $r < 0$.

Now we study the local phase portrait associated to the system (22). Basically the cases are topologically equivalent to have on the straight line $y = 0$ a center, a saddle, a center and a saddle in order from the left to the right, or the opposite order starting with a saddle. Using the symmetry $(r, y, t) \mapsto (-r, -y - t)$ is sufficient to consider $r > 0$. When the three roots of $\hat{q}(x)$ are negatives we use the symmetry $(x, \sigma, \tau, \rho, t) \mapsto (x, \sigma, \tau, \rho, t)$ and then it is sufficient to consider that the three roots are positive. If two roots of $\hat{q}(x)$ are negative and one positive, for example $\rho < \sigma < 0 < \tau$, we can consider a translation to the case $0 < \rho < \sigma < \tau$, for example the translation $x \mapsto x - \tau$ shifts the roots to $0 < \sigma - \rho < -\rho < \tau - \rho$ or renaming $0 < \hat{\rho} < \hat{\sigma} < \hat{\tau}$. Then the local phase portrait, considering the location of the equilibria, for system (22) is topologically equivalent to one in Figure 20.

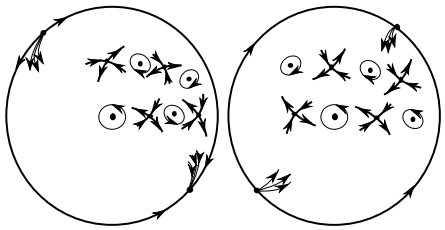

(a) (b)

FIGURE 20. Local phase portraits at the equilibria of system (3) in the case I-iv. (a) $r > 0$ and $0 < \rho < \sigma < \tau$. (b) $r > 0$ and $\rho < 0 < \sigma < \tau$.

Note that the phase portrait on Figure 20(a) are topologically equivalent to the one of Figure 20(b) (under a reflection and a translation), so we focus our study of the global phase portraits for $r > 0$ and $\rho < 0 < \sigma < \tau$.

For the global phase portrait, note that $H(x, 0)$ and $H(0, y)$ are of degree five, and the vector field, for $r >$ and $\rho < 0 < \sigma < \tau$, satisfies:

$$\dot{x}\begin{cases} > 0 & \text{if } y < 0, \\ < 0 & \text{if } 0 < y < r, \\ > 0 & \text{if } x > r, \end{cases} \quad \text{and } \dot{y}\begin{cases} > 0 & \text{if } x < \rho, \\ < 0 & \text{if } \rho < x < 0, \\ > 0 & \text{if } 0 < x < \sigma, \\ < 0 & \text{if } \sigma < x < \tau, \\ > 0 & \text{if } x > \tau, \end{cases}$$

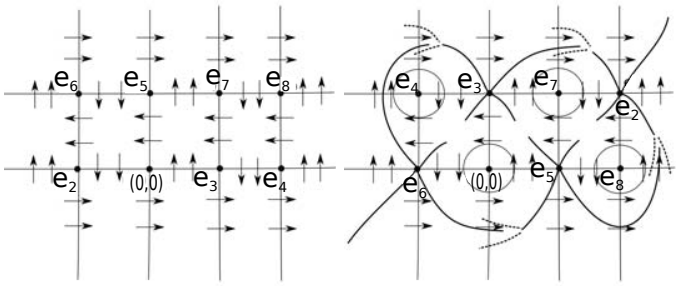

(a) (b)

FIGURE 21. The vector field (22) over the straights lines $x = 0$, $x = \rho$, $x = \sigma$, $x = \sigma$, $y = 0$ and $y = r$ if $r > 0$ and $\rho < 0 < \sigma < \tau$. (a) Vector field. (b) General analysis of the separatrices.

In Figure 21 is shown the vector field in this case over the straights lines that contains the equilibria. Following this flow we can give some general results for the separatrices. First we note that the stable separatrix of e_2 in the region $x < \rho$ and $y < 0$ must stay in this region and therefore must connect with the unstable node in V_1. The unstable separatrix of e_2 with $y < 0$ must cross the straight line $x = 0$ with $y < 0$, and its other unstable separatrix in $x < \rho$ and $y > 0$ must cross the straight line $y = r$ with $x < \rho$ and after that must cross the y-axis with $y > r$, as it is shown in Figure 21(b). On the other hand the unstable separatrix of e_8 in $x > \tau$ and $y > r$ must remain in this region connecting with the stable node at the infinity, the stable separatrix in $x < \tau$ and $y > r$ must cross the straight line $x = \sigma$ with $y > r$, and the stable separatrix in $x > \tau$ and $y < r$ must cut the x-axis with $x > \tau$ and after that must cut the straight line $x = \tau$ with $x < 0$ (see Figure 21(b)). Furthermore the unstable separatrix of e_3 in $x < 0$ must cross the straight line $x = \tau$ with $y < 0$ and after that must cross the x-axis with $x > \tau$, the stable separatrix in the same region must cut the y-axis with $y < 0$ in backward time. Finally the unstable separatrix of e_5 in the region $y > r$ must cross the straight line $x = \sigma$, and its stable separatrix in that region must cross the line $x = \rho$ with $y > r$ and after that must cut the straight line $y = r$ with $x < \rho$.

In order that we can complete the global phase portrait, we consider the level of energy on each finite saddle, here we have $h_2 = H(e_2) = (\rho^2\left(3\rho^2 - 5\rho(\sigma + \tau) + 10\sigma\tau\right))/(60\sigma\tau)$, $h_3 = H(e_3) = (\sigma^2(\sigma(3\sigma - 5\tau) - 5\rho(\sigma - 2\tau)))/(60\rho\tau)$, $h_5 = H(e_5) = (r^2(10(a^2 + b^2) - 10ar + 3r^2))/(60\left(a^2 + b^2\right))$ and it holds that and $h_8 = H(e_8) = \tau^2(-5\tau(\rho + \sigma) + 10\rho\sigma + 3\tau^2))/(60\rho\sigma) + h_5$.

Note that in system (22) we have four finite saddle, and our interest is to analyze their energy levels and possible connections, 1 case is when the four saddles are in the same energy level, if just three saddles are in the same energy level we have $4 \cdot 2$ possibles combinations, if only two saddles are in the same energy level we have $3! \cdot 6$ possibilities. The cases when all the energy level of the saddles are different provides 4! possibilities. When two pair of saddle are in the same energy level (bur not all in the same energy level) exist 6 possible relations between the energy levels of the saddles. Therefore in total we have 75 different global phase portraits for system (22). For doing an exhaustive analysis of each case we need to consider the functions $H_1(x) = h_i$ and $H_2(y) = h_i$ for $i = 2, 3, 5, 8$ every time, so the study is similar to the ones done in the proofs of statement (a) and (b) of Theorem 1 in sections 5 and 6. For this reason we do not write the global analysis. The global phase portraits for system (22) are topologically equivalent to one of the phase portraits shown in Figures 22-26.

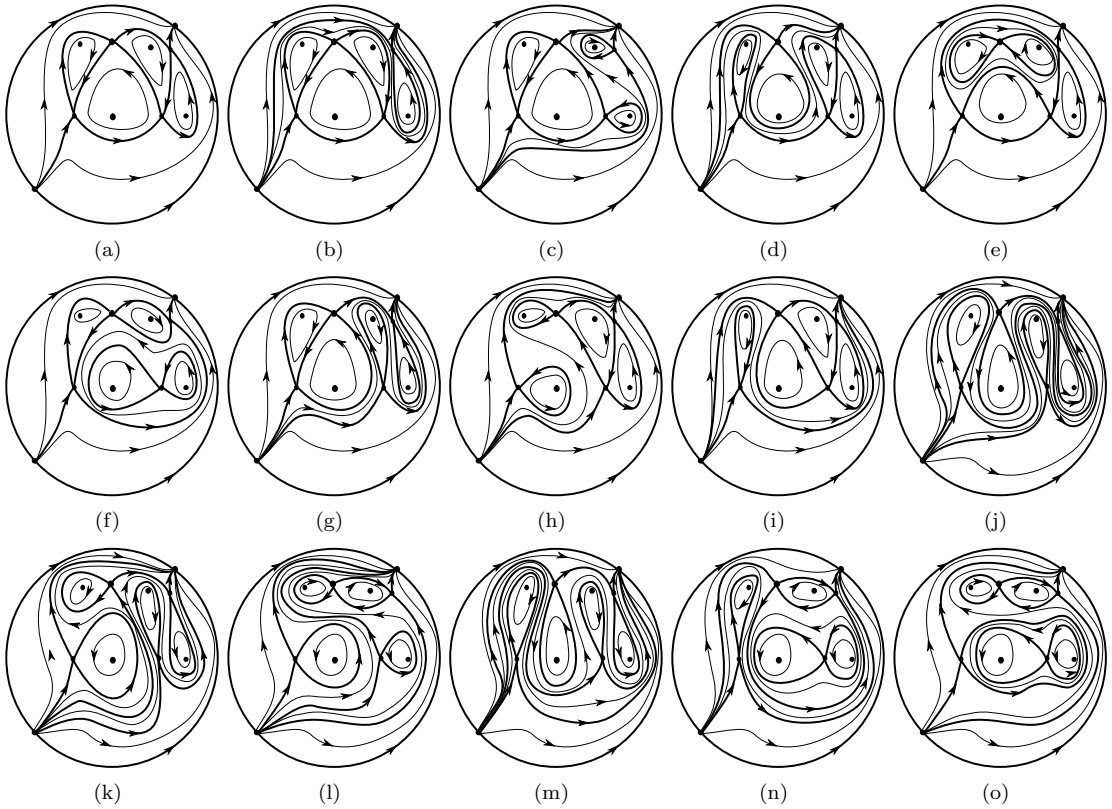

FIGURE 22. Global Phase portraits for the system (3) in the case I-iv. Here consider $r > 0$, $\rho < 0 < \sigma < \tau$. When four (a) or three saddle are in the energy level (a)-(i), $h_5 = h_8$ (j)-(o). (a) $h_2 = h_3 = h_5 = h_8$. (b) $h_8 < h_2 = h_3 = h_5$. (c) $h_2 = h_3 = h_5 < h_8$. (d) $h_5 < h_2 = h_3 = h_8$. (e) $h_2 = h_3 = h_8 < h_5$. (f) $h_3 < h_2 = h_5 = h_8$. (g) $h_2 = h_5 = h_8 < h_3$. (h) $h_2 < h_3 = h_5 = h_8$. (i) $h_3 = h_5 = h_8 < h_8$. (j) $h_5 = h_8 < h_2 < h_3$. (k) $h_2 < h_5 = h_8 < h_3$. (l) $h_2 < h_3 < h_5 = h_8$. (m) $h_5 = h_8 < h_3 < h_2$. (n) $h_3 < h_5 = h_8 < h_2$. (o) $h_3 < h_2 < h_5 = h_8$.

7.2. **Case III-iv.** We assume that $\hat{q}(x)$ has three different real roots and $\hat{p}(y)$ has a triple root r. Here the system (6) assumes the form

$$\dot{x} = -\frac{1}{r^3} y(r-y)^3, \quad \dot{y} = -\frac{1}{\rho\sigma\tau} x(x-\rho)(x-\sigma)(x-\tau). \tag{23}$$

The eight finite equilibria of system (23) are the origin, $e_2 = (0, r)$, $e_3 = (\rho, 0)$, $e_4 = (\rho, r)$, $e_5 = (\sigma, 0)$, $e_6 = (\sigma, r)$, $e_7 = (\tau, 0)$ and $e_8 = (\tau, r)$. Now we study the local phase portrait of each one, we know that the origin is a center. The equilibrium e_2 is a nilpotent equilibrium where r is a triple root of $\hat{p}(y)$, and following the notation of Lemma 4 we found that $f_1(0) > 0$, thus it is a saddle. The equilibria e_3 and e_4 are related, there are hyperbolic and we use Lemma 3 to give their local phase portrait, the first has eigenvalues $\pm\sqrt{(\rho-\sigma)(\rho-\tau)/(\sigma\tau)}$, so it is a saddle o a center. On the other hand e_4 is nilpotent, formed by a triple root and one simple root of $H_1'(x)$ and $H_2'(y)$, respectively, so it is a saddle or a center, the sign of the function $f_1(\rho)$ change in relation with the sign of $-(\rho-\sigma)(\rho-\tau))/(r^2\sigma\tau)$, more precisely is a saddle when e_3 is a center and is a center if e_3 is a saddle.

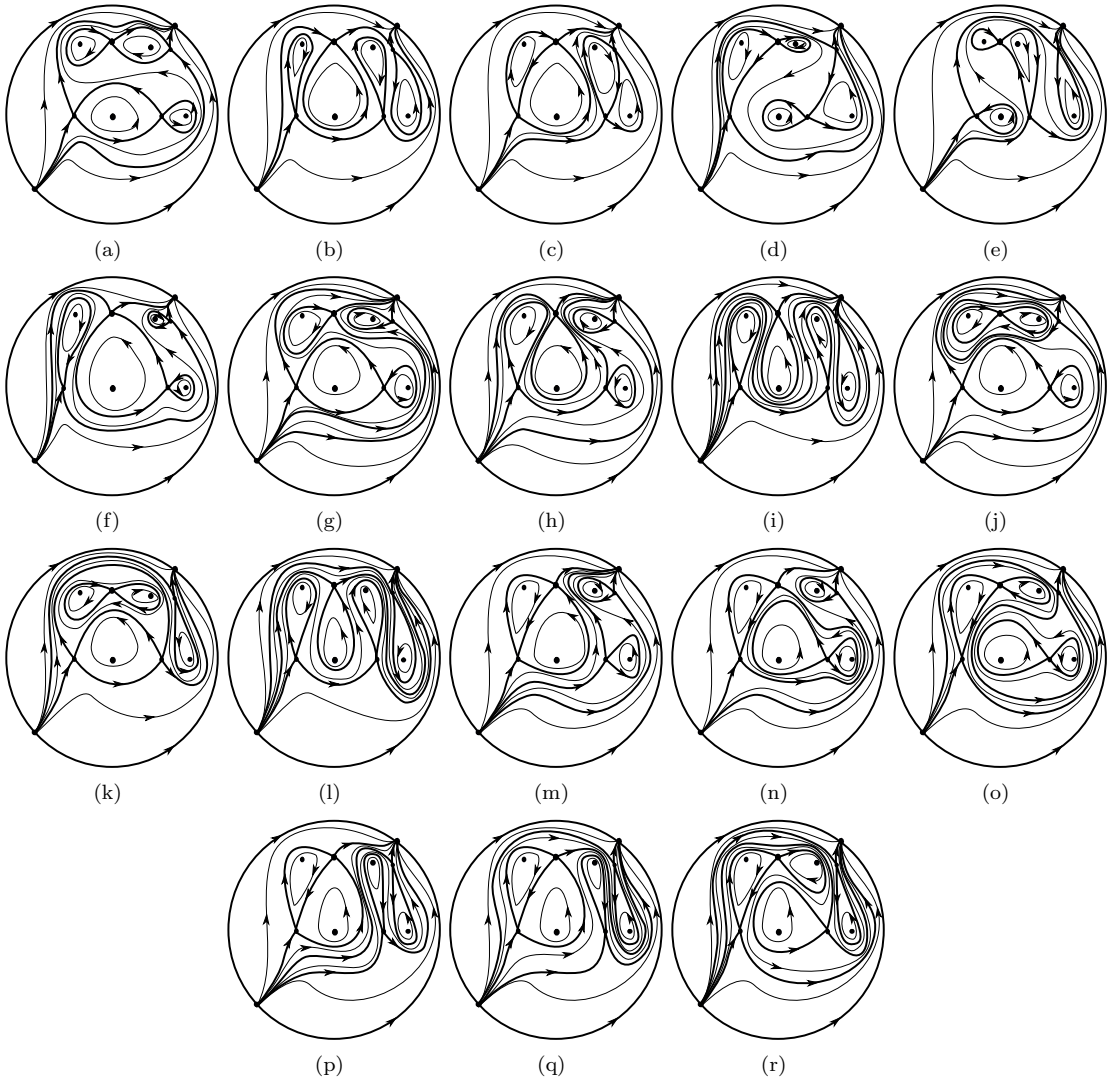

FIGURE 23. Global Phase portraits for the system (3) in case I-iv. Here consider $r > 0$, $\rho < 0 < \sigma < \tau$ when two pairs of saddle are in the same energy level (a)-(f), $r > 0$, $\rho < 0 < \sigma < \tau$ when $h_2 = h_3$ (g)-(l), and $r > 0$, $\rho < 0 < \sigma < \tau$ when $h_2 = h_5$ (m)-(r). (a) $h_2 = h_3 < h_5 = h_8$. (b) $h_2 = h_3 > h_5 = h_8$. (c) $h_2 = h_5 < h_3 = h_8$. (d) $h_2 = h_5 > h_3 = h_8$. (e) $h_2 = h_8 < h_3 = h_5$. (f) $h_2 = h_8 > h_3 = h_5$. (g) $h_2 = h_3 < h_5 < h_8$. (h) $h_5 < h_2 = h_3 < h_8$. (i) $h_5 < h_8 < h_2 = h_3$. (j) $h_2 = h_3 < h_8 < h_5$. (k) $h_8 < h_2 = h_3 < h_5$. (l) $h_8 < h_5 < h_2 = h_3$. (m) $h_2 = h_5 < h_3 < h_8$. (n) $h_3 < h_2 = h_5 < h_8$. (o) $h_3 < h_8 < h_2 = h_5$. (p) $h_2 = h_5 < h_8 < h_3$. (q) $h_8 < h_2 = h_5 < h_3$. (r) $h_8 < h_3 < h_2 = h_5$.

The equilibria e_5 and e_6 have the same relation that e_3 and e_4. In fact the eigenvalues of the hyperbolic equilibria e_5 are $\pm\sqrt{-(\rho-\sigma)(\sigma-\tau)/(\rho\tau)}$, and e_6 is nilpotent, by Lemma 4 it is a saddle or a center, it depends on $(\rho-\sigma)(\sigma-\tau))/(\rho\tau)$. And in a similar way these relations happen for e_7 and e_8, because the

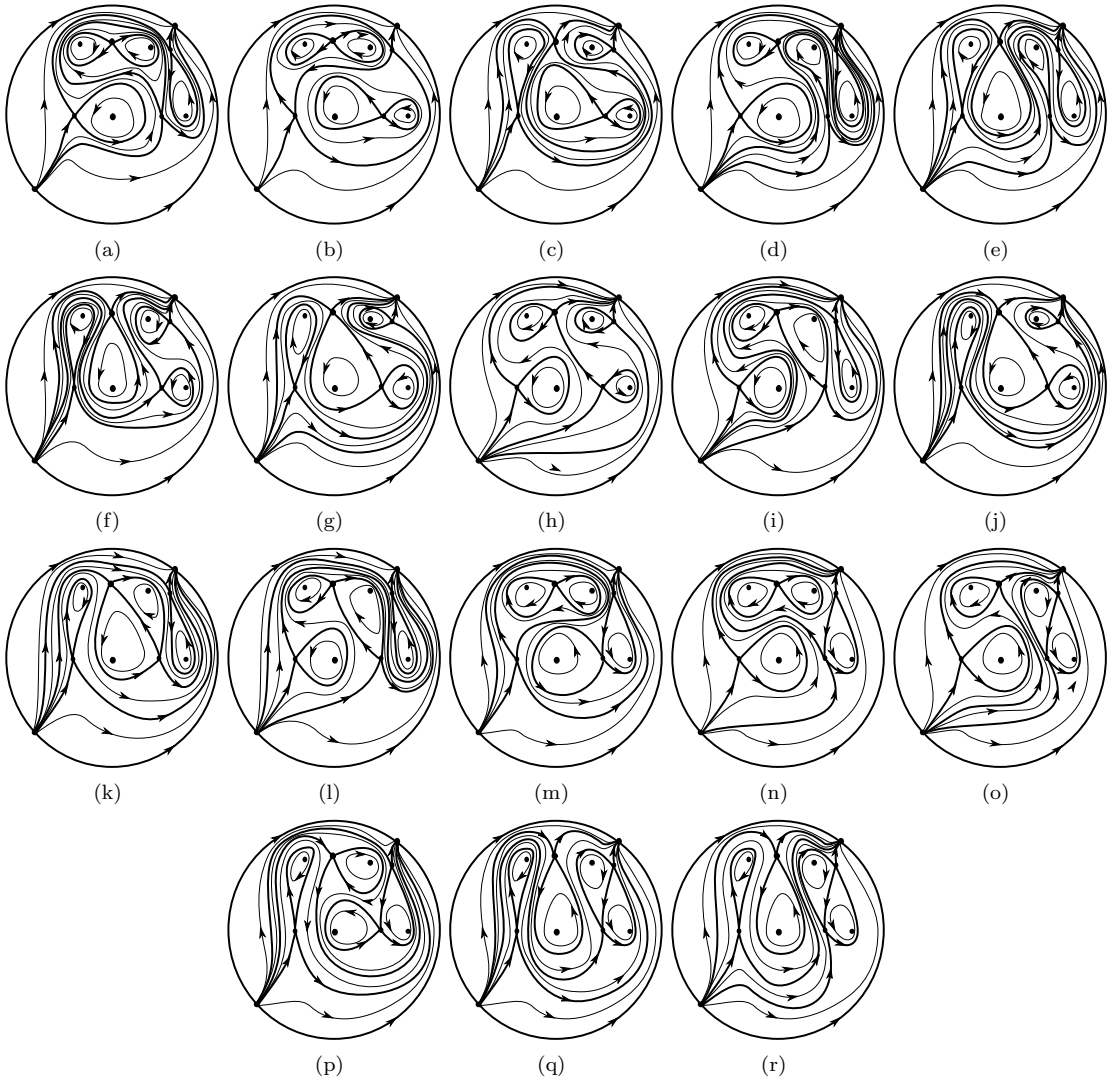

FIGURE 24. Global Phase portraits for the system (3) in the case I-iv. Here consider $r > 0$, $\rho < 0 < \sigma < \tau$ when $h_2 = h_8$ (a)-(f), $h_3 = h_5$ (g)-(l) and $h_3 = h_8$ (m)-(r). (a) $h_2 = h_8 < h_3 < h_5$. (b) $h_3 < h_2 = h_8 < h_5$. (c) $h_3 < h_5 < h_2 = h_8$. (d) $h_2 = h_8 < h_5 < h_3$. (e) $h_5 < h_2 = h_8 < h_3$. (f) $h_5 < h_3 < h_2 = h_8$. (g) $h_3 = h_5 < h_2 < h_8$. (h) $h_2 < h_3 = h_5 < h_8$. (i) $h_2 < h_8 < h_3 = h_5$. (j) $h_3 = h_5 < h_8 < h_2$. (k) $h_8 < h_3 = h_5 < h_2$. (l) $h_8 < h_2 < h_3 = h_5$. (m) $h_3 = h_8 < h_2 < h_5$. (n) $h_2 < h_3 = h_8 < h_5$. (o) $h_2 < h_5 < h_3 = h_8$. (p) $h_3 = h_8 < h_5 < h_2$. (q) $h_5 < h_3 = h_8 < h_2$. (r) $h_5 < h_2 < h_3 = h_8$.

eigenvalues of e_7 are $\pm\sqrt{(\rho-\tau)(\sigma-\tau)/(\rho\sigma)}$, and e_8 is nilpotent and its local phase portrait is a saddle or a center according to the sign of $-(\rho-\tau)(\sigma-\tau)/(\rho\sigma)$.

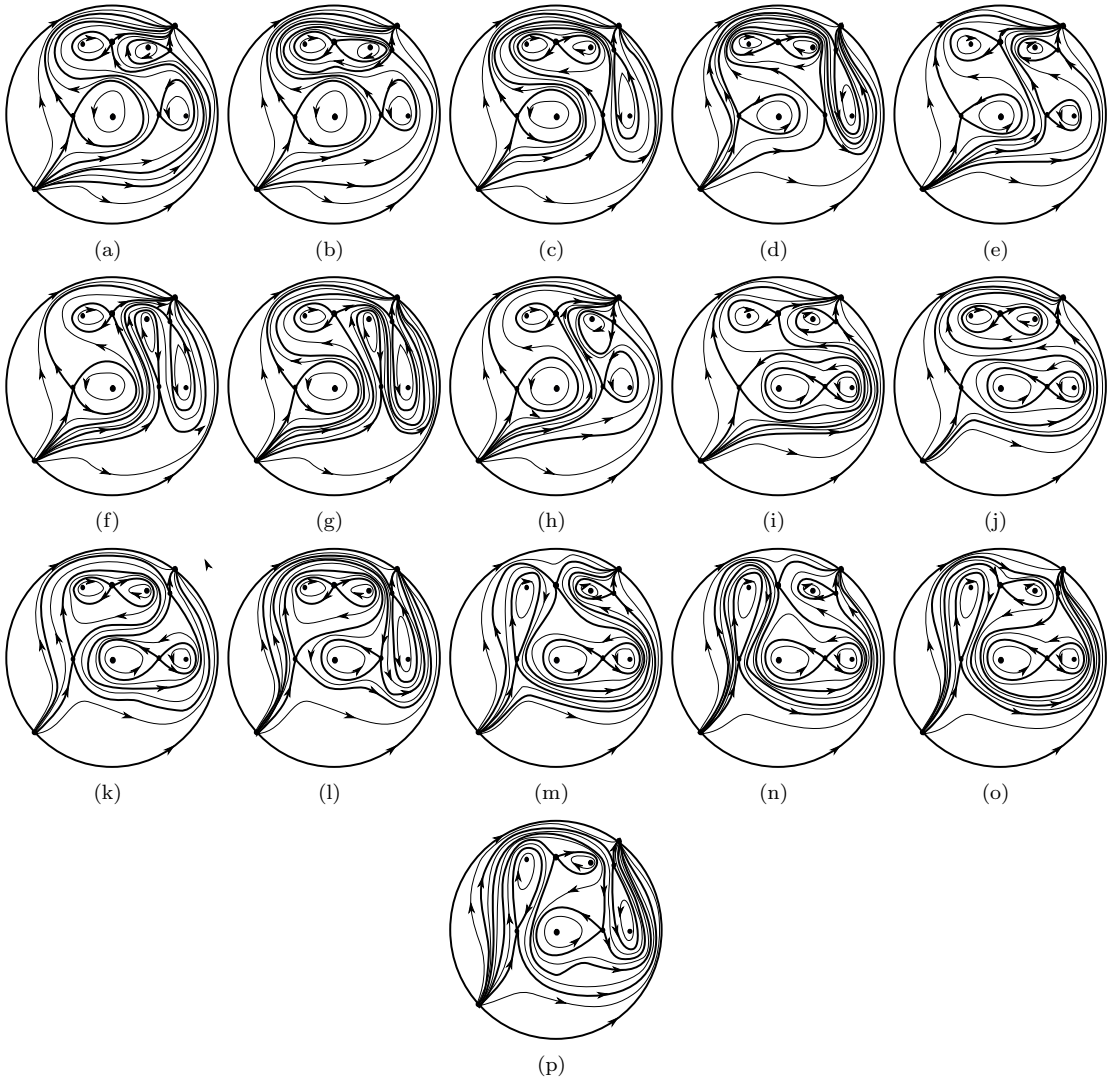

FIGURE 25. Global Phase portraits for the system (3) in the case I-iv. Here consider $r > 0$, $\rho < 0 < \sigma < \tau$ when $h_2 < h_3 < h_5$ (a)-(d), $h_2 < h_5 < h_3$ (e)-(h), $h_3 < h_2 < h_5$ (i)-(l), and $h_3 < h_5 < h_2$ (m)-(p). (a) $h_2 < h_3 < h_5 < h_8$. (b) $h_2 < h_3 < h_8 < h_5$. (c) $h_2 < h_8 < h_3 < h_5$. (d) $h_8 < h_3 < h_3 < h_5$. (e) $h_2 < h_5 < h_3 < h_8$. (f) $h_2 < h_5 < h_8 < h_3$. (g) $h_2 < h_8 < h_5 < h_3$. (h) $h_8 < h_2 < h_5 < h_3$. (i) $h_3 < h_2 < h_5 < h_8$. (j) $h_3 < h_2 < h_8 < h_5$. (k) $h_3 < h_8 < h_2 < h_5$. (l) $h_8 < h_3 < h_2 < h_5$. (m) $h_3 < h_5 < h_2 < h_8$. (n) $h_3 < h_5 < h_8 < h_2$. (o) $h_3 < h_8 < h_5 < h_2$. (p) $h_8 < h_3 < h_5 < h_2$.

In the infinity the equilibrium P is an unstable node for $r < 0$, or a stable node for $r > 0$. Considering the symmetries given in case I-iv, we arrive that the local phase portraits for case III-iv are topologically equivalent to the ones of Figure 20.

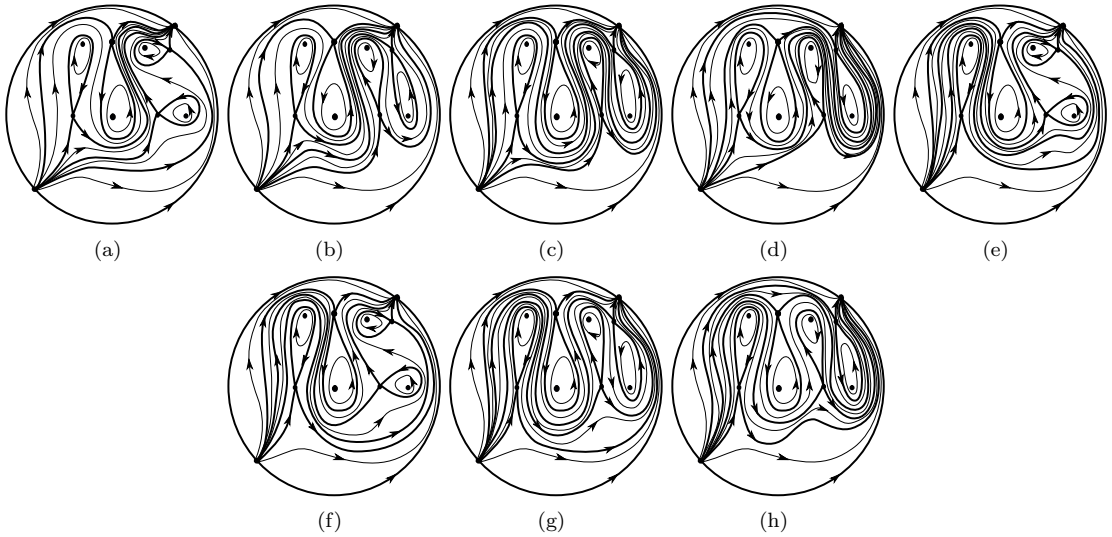

FIGURE 26. Global Phase portraits for the system (3) in the case I-iv. Here consider $r > 0$, $\rho < 0 < \sigma < \tau$ when all the saddle are in different energy level and its satisfy $h_5 < h_2 < h_3$ (a)-(d), $h_5 < h_3 < h_2$ (e)-(h). (a) $h_5 < h_2 < h_3 < h_8$. (b) $h_5 < h_2 < h_8 < h_3$. (c) $h_5 < h_8 < h_2 < h_3$. (d) $h_8 < h_5 < h_2 < h_3$. (e) $h_5 < h_3 < h_2 < h_8$. (f) $h_5 < h_3 < h_8 < h_2$. (g) $h_5 < h_8 < h_3 < h_2$. (h) $h_8 < h_5 < h_3 < h_2$.

For studying the global phase portraits, noting that the local phase portraits coincide with the ones of case I-iv, we consider the energy level $h_i = H(e_i)$, which in this case are $h_2 = r^2/10$, $h_3 = \rho^2\left(3\rho^2 - 5\rho(\sigma+\tau) + 10\sigma\tau\right)/(60\sigma\tau)$, $h_5 = \sigma^2(\sigma(3\sigma-5\tau)-5\rho(\sigma-2\tau))/(60\rho\tau)$, and $h_8 = h_2+\tau^2(-5\tau(\rho+\sigma)+10\rho\sigma+3\tau^2)/(60\rho\sigma)$, the phase portraits of system (23) are topologically equivalent to one of the 67 phase portraits in Figures 22-26.

Thus we have completed the proof of Theorem 1 statement (c).

8. Proof of Theorem 1 statement (d)

We consider $\hat{p}(y)$ and $\hat{q}(x)$ having both two different real roots, one of them with multiplicity two. This happens in the case II-ii. Thus we consider that the polynomial $\hat{p}(y)$ has one simple real root r and one double real root s, and the polynomial $\hat{q}(x)$ has one simple real root ρ and one double real root σ. Then system (3) becomes

$$\dot{x} = \frac{1}{rs^2}y(y-r)(y-sy)^2, \quad \dot{y} = -\frac{1}{\rho\sigma^2}x(x-\rho)(x-\sigma)^2. \tag{24}$$

This system has nine finite equilibria, namely $e_1 = (0,0)$, $e_2 = (0,r)$, $e_3 = (0,s)$, $e_4 = (\rho,0)$, $e_5 = (\rho,r)$, $e_6 = (\rho,s)$, $e_7 = (\sigma,0)$, $e_8 = (\sigma,r)$ and $e_9 = (\sigma,s)$. The origin is a center as we know, other three equilibria are hyperbolic and by Lemma 3 we have their local phase portrait: e_2 is a saddle with eigenvalues $\pm(1-r/s)$, e_4 is a saddle too with eigenvalues $\pm(1-\rho/\sigma)$, and e_5 is a center with eigenvalues $\pm\sqrt{-1}((r-s)(\rho-\sigma))/(s\sigma)$.

Four finite equilibria e_3, e_6, e_7 and e_8 are nilpotent . These four nilpotent equilibria are composed for one double root of $H_1'(x)$ or $H_2'(y)$, so all of them are cusps according to Lemma 4. Furthermore for

example for the equilibria e_3 and e_4, a complete analysis gives the direction of the flow in relation to the coefficient $(r-s)/(rs)$. Figure 27 shows the possibilities for $r>0$.

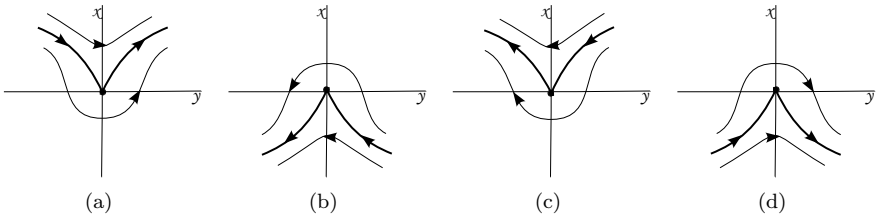

FIGURE 27. Local phase portraits for the nilpotent equilibria e_3 and e_6 in the case I-iv for $r>0$ shifted to the origin. (a) e_3 when $-(r-s)/(rs)>0$. (b) e_3 when $-(r-s)/(rs)<0$. (c) e_6 when $(r-s)/(rs)>0$. (d) e_6 when $(r-s)/(rs)<0$.

Finally the equilibrium e_9 is degenerate, where s is a double root of $H_2'(y)$ and σ is a double root of $H_1'(x)$, thus by Lemma 5 the equilibrium consists in two hyperbolic sectors. Figure 28 shows the different directions and sense of the separatrices in function of the signs of $(r-s)/(rs)$ and of $(\rho-\sigma)/(\rho\sigma)$.

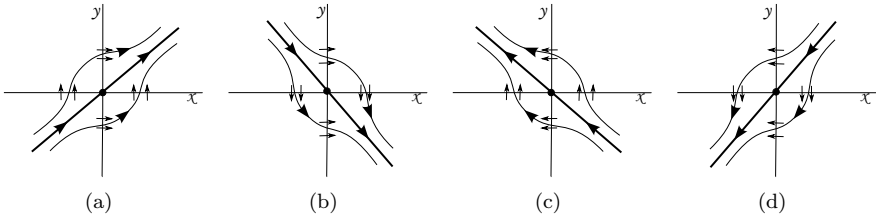

FIGURE 28. Local phase portrait at the equilibrium $e_9=(\sigma,s)$ of system (24) after translation to the origin. (a) $(r-s)/(rs)>0$ and $(\rho-\sigma)/(\rho\sigma)>0$. (b) $(r-s)/(rs)>0$ and $(\rho-\sigma)/(\rho\sigma)<0$. (c) $(r-s)/(rs)<0$ and $(\rho-\sigma)/(\rho\sigma)>0$. (d) $(r-s)/(rs)<0$ and $(\rho-\sigma)/(\rho\sigma)<0$.

Thus we have the local phase portraits of all the finite equilibrium points. At the infinite, we have that the equilibrium P is a stable node if $r>0$ and is an unstable node if $r<0$.

The symmetries $(y,r,s,t)\mapsto(-y,-r,-s,-t)$ and $(x,\rho,\sigma,\tau)\mapsto(-x,-\rho,-\sigma,-\tau)$ reduce the study to the cases $0<r<s$, or $0<s<r$, or $r<0<s$ and $0<\rho<\sigma$, $0<\sigma<\rho$ or $\rho<0<\sigma$, combining the first three cases with the last three cases we have in total 9 cases. But these cases can be reduced by reflections and translations to 5 cases, for example the case $0<r<s$ and $0<\sigma<\rho$ through the change of variables $(x,y)\mapsto(-x+r,y-\rho)$ is equivalent to case $0<s<r$ and $0<\rho<\sigma$. So the local phase portrait considering the location of the equilibria are topologically equivalent to one of the 5 local phase portraits in Figure 29.

The global phase portrait now have many possibilities. Note that there exist 7 finite equilibria with separatrices, so doing a complete analysis of the possible separatrices connections of these equilibria implies study at least 7! different possibilities, this implies that the analysis will be huge and the ideas for studying each case follow the same arguments used in the proof of statement (a), (b) and (c) of Theorem 1. For this reason we prefer omit the analysis of the global phase portrait for statement (d).

As a comment note that for the finite equilibria with separatrices we have that the level of energy $h_i=H(e_i)$ are: $h_2=(r^2(3r^2-10rs+10s^2))/(60s^2)>0$, $h_3=((5r-2s)s^2)/(60r)$, $h_4=\rho^2(3\rho^2-10\rho\sigma+$

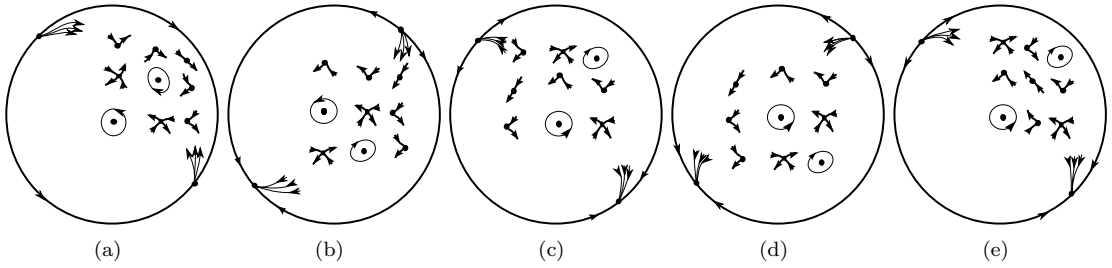

FIGURE 29. Local phase portraits at the equilibria of system (3) in the case II-ii. (a) $0 < r < s$ and $0 < \rho < \sigma$. (b) $r < 0 < s$ and $0 < \rho < \sigma$. (c) $0 < s < r$ and $\sigma < 0 < \rho$. (d) $r < 0 < s$ and $\sigma < 0 < \rho$. (e) $0 < s < r$ and $0 < \sigma < \rho$.

$10\sigma^2)/(60\sigma^2) > 0$, $h_5 = h_2 + h_4$, $h_6 = h_3 + h_4$, $h_7 = \sigma^2(5\rho - 2\sigma)/(60\rho)$, $h_8 = h_2 + h_7$ and $h_9 = h_3 + h_7$. And observe that $h_2 < h_5$ and $h_4 < h_5$.

9. Proof of Theorem 1 statement (e)

We consider that $\hat{p}(y)$ (respectively $\hat{q}(x)$) has two different real roots, one with multiplicity two and $\hat{q}(x)$ (respectively $\hat{p}(y)$) has three different real roots, this happens in cases II-iv and IV-ii. From Remark 2 it is sufficient to study the case II-iv.

Considering that the polynomial $\hat{q}(x)$ has three different real roots ρ, σ and τ, the simple root of $\hat{p}(y)$ is r and the double root of $\hat{p}(y)$ is s, then system (6) becomes

$$\dot{x} = \frac{1}{rs^2} y(y-r)(y-s)^2, \quad \dot{y} = -\frac{1}{\rho\sigma\tau} x(x-\rho)(x-\sigma)(x-\tau). \tag{25}$$

Since $\hat{q}(x)$ has three different real roots, and $\hat{p}(y)$ has two different real roots, system (25) has twelve finite equilibria. Following Lemma 3 we can give the behavior of the hyperbolic equilibria. The origin is a center, and there exist a saddle in $e_2 = (0, r)$ beause their eigenvalues are $\pm(1 - r/s)$. There exist three pairs of finite equilibria where one is a saddle and other is a center under convenient conditions, the first par of equilibria is $e_4 = (\rho, 0)$ and $e_5 = (\rho, r)$, the eigenvalues for $(\rho, 0)$ are $\pm\sqrt{(\rho-\sigma)(\rho-\tau)/(\sigma\tau)}$, and for (ρ, r) are $\pm(r-s)/s\ \sqrt{-(\rho-\sigma)(\rho-\tau)/(\sigma\tau)}$.

A second pair with saddle and center is $e_7 = (\sigma, 0)$ and $e_8 = (\sigma, r)$ with eigenvalues associated $\pm\sqrt{-(\rho-\sigma)(\sigma-\tau)/(\rho\tau)}$ and $\pm(s-r)/s\sqrt{(\rho-\sigma)(\sigma-\tau)/(\rho\tau)}]$, respectively. The last pair of saddle-center is $e_{10} = (\tau, 0)$, and $e_{11} = (\tau, r)$ which eigenvalues are $\pm\sqrt{(\rho-\tau)(\sigma-\tau)/(\rho\sigma)}$, and $\pm(r-s)/s[(\rho-\tau)(\sigma-\tau)/(\rho\sigma)]^{1/2}$, respectively.

The other four finite equilibria are $e_3 = (0, s)$, $e_6 = (\rho, s)$, $e_9 = (\sigma, s)$ and $e_{12} = (\tau, s)$, they are nilpotent. By Lemma 4 (since s is double root of $H_2'(y)$) we conclude that these four equilibria are cusps.

The equilibria on the straight line $y = 0$ and on $y = r$ are always two saddles and two centers and they are positioned interchanged. Thus, we have completed the study of the local phase portraits for every finite equilibrium point.

On the infinity we have that the infinite equilibria P is a stable node if $r > 0$ and an unstable node if $r < 0$.

Following the results of finite and infinite equilibria, the local phase portrait of all the equilibrium points are shown in the Poincaré disc in Figure 30. It is only necessary to study the cases when all the roots are

positives, and the relation between the root r and s of $\hat{p}(y)$. This is due to the symmetries that system (25) presents, for example if the roots are all negatives we can apply the changes $(y, r, s, t) \to (-y, -r, -s, -t)$ and $(y, \rho, \sigma, \tau, t) \to (-y, -\rho, -\sigma, -\tau, -t)$.

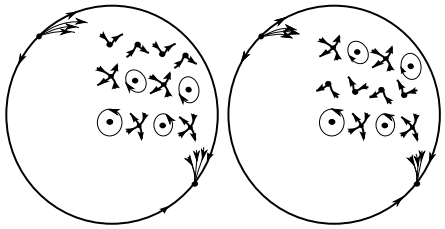

(a) (b)

FIGURE 30. Local phase portraits at the equilibria of system (3) in the case II-iv. (a) if $0 < r < s$. (b) if $0 < s < r$.

We provide the levels of energy of the finite equilibria $h_i = H(e_i)$, $i = \overline{1-12}$, these are $h_1 = 0$, $h_2 = (r^2(3r^2 - 10rs + 10s^2))/(60s^2)$, $h_3 = ((5r - 2s)s^2)/(60r)$, $h_4 = \rho^2(3\rho^2 - 5\rho(\sigma + \tau) + 10\sigma\tau)/(60\sigma\tau)$, $h_5 = h_2 + h_4$, $h_6 = h_3 + h_4$, $h_7 = \sigma^2(\sigma(3\sigma - 5\tau) - 5\rho(\sigma - 2\tau))/(60\rho\tau)$, $h_8 = h_2 + h_7$, $h_9 = h_3 + h_7$, $h_{10} = \tau^2(-5\tau(\rho + \sigma) + 10\rho\sigma + 3\tau^2)/(60\rho\sigma)$, $h_{11} = h_2 + h_{10}$ and $h_{12} = h_3 + h_{10}$.

The analysis of the global phase portraits must take into account the connections between the separatrices of saddles and cusps. The quantity of possibilities is more than 8! so their study is tedious. For this reason we prefer only to give the local phase portrait on the Poincaré disc.

10. Proof of Theorem 1 statement (f)

In this last case we have that $\hat{p}(y)$ and $\hat{q}(x)$ have three different real roots, i.e. we are in the case IV-iv.

Suppose that the roots of $\hat{q}(x)$ are ρ, σ and τ, and the three different real roots of $\hat{p}(y)$ are r, s and l. Then the associated system is

$$\dot{x} = \frac{1}{rsl} y(y - r)(y - s)(y - l), \quad \dot{y} = -\frac{1}{\rho\sigma\tau} x(x - \rho)(x - \sigma)(x - \tau).$$

This case has more finite equilibria, in total 16 finite equilibria. We proceed to detail each one and study their stability, all the equilibria are hyperbolic, so we apply Lemma 3. The trivial equilibrium is the center at the origin. All the other equilibria are centers or saddles and their local phase portrait depend on the parameters r, s, l, ρ, σ and τ. A second equilibrium is $e_2 = (0, r)$ whose eigenvalues are $\lambda_2^{\pm} = \pm\sqrt{(r - s)(r - l)/(sl)}$, so it is a saddle or a center. Other equilibria on $x = 0$ is $e_3 = (0, s)$ and it is a saddle or a center because their eigenvalues are $\lambda_3^{\pm} = \pm\sqrt{(s - r)(s - l)/(rl)}$. A fourth equilibria on the y-axis is $e_4 = (0, l)$ and it is a saddle or a center too with eigenvalues $\lambda_4^{\pm} = \pm\sqrt{(r - l)(s - l)/(rs)}$.

On the straight line $x = \rho$ we have four equilibria, centers or saddles, $e_5 = (\rho, 0)$ with eigenvalues $\lambda_5^{\pm} = \pm\sqrt{(\rho - \sigma)(\rho - \tau)/(\sigma\tau)}$, a sixth equilibrium is $e_6 = (\rho, r)$ and their stability conditions depend of sign of λ_2 and λ_5 because their eigenvalues are $\pm i\lambda_2\lambda_5$, $e_7 = (\rho, s)$ is a saddle or center that depends on λ_3 and λ_5 because their eigenvalues are $\pm i\lambda_3\lambda_5$, the other equilibria on $x = \rho$ is $e_8 = (\rho, l)$ with eigenvalues $\pm i\lambda_4\lambda_5$.

There exist four equilibria on $x = \sigma$, these are $e_9 = (\sigma, 0)$ with eigenvalues $\lambda_9^{\pm} = \pm\sqrt{(\sigma - \rho)(\sigma - \tau)/(\rho\tau)}$, $e_{10} = (\sigma, r)$ with eigenvalues $\pm i\lambda_2\lambda_9$, $e_{11} = (\sigma, s)$ with eigenvalues $\pm i\lambda_3\lambda_9$, and $e_{12} = (\sigma, l)$ with eigenvalues $\pm i\lambda_4\lambda_9$.

And the last four finite equilibria are on $x = \tau$ and they are $e_{13} = (\tau, 0)$ with eigenvalues $\lambda_{13}^{\pm} = \pm\sqrt{(\rho-\tau)(\sigma-\tau)/(\rho\sigma)}$, $e_{14} = (\tau, r)$ with eigenvalues $\pm i\lambda_2\lambda_{13}$, $e_{15} = (\tau, s)$ with eigenvalues $\pm i\lambda_3\lambda_{13}$ and finally $e_{16} = (\tau, l)$ with eigenvalues $\pm i\lambda_4\lambda_{13}$. The study of the eigenvalues of the equilibria on the axis gives the information that over each axis there exist two saddles and two centers, the local phase portrait of the other finite equilibria depends on these seven equilibria that are on the axes.

The infinite equilibria P is a stable node if $rst > 0$ and it is an unstable node if $rst < 0$.

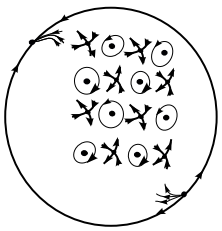

FIGURE 31. Local phase portraits for system (3) in the case IV-iv if $0 < r < s < t$ and $0 < \rho < \sigma < \tau$.

We observe that it is sufficient to study the case $0 < r < s < t$ and $0 < \rho < \sigma < \tau$, the other cases are similar. This is due to the symmetries $(y, r, s, l, t) \to (-y, -r, -s, -l, -t)$ and $(x, \rho, \sigma, \tau, t) \to (-x, -\rho, -\sigma, -\tau, -t)$. If two roots of $\hat{p}(y)$ and/or $\hat{q}(x)$ are negative we do a translation to the origin to equilibrium (x^*, y^*) such that $x^* < \tilde{x}$ and $y^* < \tilde{y}$ for every $(\tilde{x}, \tilde{y})$ finite equilibria. And if a unique root of $\hat{p}(y)$ and/or $\hat{q}(x)$ is negative we can do a reflection with respect to the y-axis and apply the translation previously defined. In this case $e_2, e_4, e_5, e_7, e_{10}, e_{12}, e_{13}$ and e_{15} are saddles and the other finite equilibria are centers, as shown in Figure 31. Here we have 8 saddles, so the study of the connections between their separatrices if tedious, and follow the arguments used in the proof of the global phase portraits for systems associated to statement (a), (b) and (c) of Theorem 1.

The complete study of the phase portraits stated in Theorem 1 is proved.

11. Concluding remarks

In this work we analyze the global phase portraits associated to the autonomous Hamiltonian systems with one degree of freedom whose Hamiltonian function is

$$H(x, y) = \frac{1}{2}(x^2 + y^2) + \frac{a_3}{3}x^3 + \frac{a_4}{4}x^4 + \frac{a_5}{5}x^5 + \frac{b_3}{3}y^3 + \frac{b_4}{4}y^4 + \frac{b_5}{5}y^5,$$

which depends on six real parameters. It is observed that the equilibrium points in the finite part can be centers, saddles, cusps or the union of two hyperbolic sectors, and in the infinite part can be nodes. The number of finite equilibria depends on the number of distinct real roots of the polynomial H_x and H_y, and in the infinity there are exactly two equilibrium points. The type of the equilibria (hyperbolic, nilpotent or degenerate) and the difficulty for their study depends on the multiplicity of the root that provides the equilibrium, a higher multiplicity means higher difficulty. The main difficulty in order to classify the global phase portrait is the analysis of the possible connections of the separatrices between the equilibria. In fact in some situations there are several possibilities of connections (see for example the case II-iv or IV-iv). Of course, the complexity of the global description is associated to the type of the distinct real roots of the polynomials H_x and H_y and the energy levels of the saddle equilibrium points. More precisely, if there is only one real root of H_x and one real root of H_y (besides of the trivial in each case) we have an easy situation for characterizing the connections of the separatrices, here only exist two saddles and the most simple separatrix configuration happens when they are on the same energy level, this

means that the parameters of the Hamiltonian satisfy certain conditions. While if one of the polynomials H_x or H_y present four different real root and the other polynomial only one real root (case I-iv and III-iv) we have the most difficult situation because there are 75 possibilities for the possible connections of the separatrices of the finite saddles and the infinite nodes. Note that when there exist another type of finite equilibria with separatrices, cusps or the union of two hyperbolic sectors, this analysis becomes more hard. An important argument used for the description of the global phase portraits is the analysis of the auxiliary functions $\mu_i(x) = h_i - H_1(x)$ and $\nu(y) = h_i - H_2(y)$ where h_i is the energy level of the finite equilibria, our interest is in the equilibria which present separatrices. Finally in the case where the global analysis, related to the separatrix and the canonical region of the Poincaré disc give a big number of possibilities, we only describe the local phase portrait at every equilibria, and some general results for the global phase portraits.

Acknowledgements

J. Llibre is partially supported by MINECO-FEDER grant MTM2016-77278-P, a MINECO grant MTM2013-40998-P, and an AGAUR grant number 2014SGR-568. Y. Paulina Martínez was supported by a CONICYT fellowship (Chile). C. Vidal was partially supported by CONICYT (Chile) through FONDECYT project 1130644. This paper is part of Y. Paulina Martínez Ph.D. thesis in the Program Doctorado en Matemática Aplicada, Universidad del Bío-Bío (Chile).

References

[1] A.A. Andronov, A.A. Vitt and S.E. Khaikin, *Theory of Oscillators*, Dover Publications Inc., New York, 1987. Translated form the Russian by F. Immirzi, Reprint of the 1966 translation.

[2] V. I. Arnold and Y. S. Ilyashenko, *Dynamical Systems I, Ordinary Differential Equations". Encyclopaedia of Mathematical Sciences*, Vols **1**–**2**, Springer-Verlag, Heidelberg, 1988.

[3] J.C. Artés and J. Llibre, *Quadratic Hamiltonian vector fields*, J. Differential Equations **107** (1994), 80–95.

[4] N.N. Bautin, *On the number of limit cycles which appear with the variation of coefficients from an equilibrium position of focus or center type*, Mat. Sb. **30** (1952), 181–196; Mer. Math. Soc. Transl. **100** (1954), 1–19.

[5] J. Chavarriga and J. Giné, *Integrability of a linear center perturbed by a fourth degree homogeneous polynomial*, Publ. Mat. **40** (1996), 21–39.

[6] J. Chavarriga and J. Giné, *Integrability of a linear center perturbed by a fifth degree homogeneous polynomial*, Publ. Mat. **41** (1997), 335–356.

[7] I. Colak, J. Llibre and C. Valls, *Hamiltonian nilpotent centers of linear plus cubic homogeneous polynomial vector fields*, Adv. Math. **259** (2014), 655–687.

[8] I. Colak, J. Llibre and C. Valls, *Hamiltonian linear type centers of linear plus cubic homogeneous polynomial vector fields*, J. Differential Equations **257** (2014), 1623–1661.

[9] I. Colak, J. Llibre and C. Valls, *Bifurcations diagrams for Hamiltonian linear type centers of linear plus cubic homogeneous polynomial vector fields*, J. Differential Equations **258** (2015), 846–879.

[10] I. Colak, J. Llibre and C. Valls, *Bifurcations diagrams for nilpotent centers of linear plus cubic homogeneous polynomial vector fields*, J. Differential Equations **262** (2017), 5518–5533.

[11] H. Dulac, *Détermination et integration dâune certaine classe dâéquations différentielle ayant par point singulier un centre*, Bull. Sci. Math. Sér. (2) **32** (1908), 230–252.

[12] F. Dumortier, J. Llibre and J.C. Artés, *Qualitative theory of planar differential systems*, Universitext, Spring-Verlag, 2006.

[13] H. Goldstein, *Classical Mechanics*, Addison-Wesley Press, Inc., Cambridge, Mass, 1951.

[14] A. Guillamon and C. Pantazi, *Phase portraits of separable Hamiltonian systems*, Nonl. Analysis **74** (2011), 4012-4035.

[15] W. Kapteyn, *On the midpoints of integral curves of differential equations of the first Degree*, Nederl. Akad. Wetensch. Verslag Afd. Natuurk. Konikl. Nederland (1911), 1446–1457 (in Dutch).

[16] W. Kapteyn, *New investigations on the midpoints of integrals of differential equations of the first degree*, Nederl. Akad. Wetensch. Verslag Afd. Natuurk. **20** (1912), 1354–1365; Nederl. Akad. Wetensch. Verslag Afd. Natuurk. **21** (1913), 27–33 (in Dutch).

[17] J.H. Kim, S.W. Lee, H. Massen and H.W. Lee, *Relativistic oscillator of constant period*, Phys. Rev. A **53** (1996), 2991–2997.

[18] K.E. Malkin, *Criteria for the center for a certain differential equation*, Vols. Mat. Sb. Vyp. **2** (1964), 87–91 (in Russian).
[19] L. Markus, *Global structure of ordinary differential equations in the plane:* Trans. Amer. Math Soc. **76** (1954), 127–148.
[20] Y.P. Martínez, C. Vidal, *Classification of global phase portraits and bifurcation diagrams of Hamiltonian systems with rational potential*, J. Diff. Equation **261** (2016), 5923–5948.
[21] D. A. Neumann, *Classification of continuous flows on 2–manifolds*, Proc. Amer. Math. Soc. **48** (1975), 73–81.
[22] M.M. Peixoto, *Dynamical Systems. Proccedings of a Symposium held at the University of Bahia*, 389–420, Acad. Press, New York, 1973.
[23] H. Poincaré, *Mémoire sur les courbes définies par les équations différentielles*, Journal de Mathématiques **37** (1881), 375–422; Oeuvres de Henri Poincaré, vol. I, Gauthier-Villars, Paris, 1951, pp 3–84.
[24] H. Stommel *Trajectories of small bodies sinking slowly through convection cells*, J. Mar. Res. **8** (1949), 24–29.
[25] N.I. Vulpe, *Affine-invariant conditions for the topological discrimination of quadratic systems with a center*, Differential Equations **19** (1983), 273–280.
[26] N.I. Vulpe and K.S. Sibirskii, *Centro-affine invariant conditions for the existence of a center of a differential system with cubic nonlinearities*, Dokl. Akad. Nauk. SSSR **301** (1988), 1297–1301 (in Russian); translation in: Soviet Math. Dokl. **38** (1989), 198–201.

(J. Llibre) Departament de Matemàtiques, Facultat de Ciències Universitat Autònoma de Barcelona, 08193 Bellaterra, Barcelona, Catalonia, Spain

E-mail address: jllibre@mat.uab.cat

(Y.P. Martínez) Departamento de Matemática, Facultad de Ciencias, Universidad del Bío-Bío, Casilla 5–C, Concepción, VIII–Región, Chile

E-mail address: ymartinez@ubiobio.cl

(C. Vidal) Departamento de Matemática, Facultad de Ciencias, Universidad del Bío-Bío, Casilla 5–C, Concepción, VIII–región, Chile

E-mail address: clvidal@ubiobio.cl